Excess-entropy scaling

Jeppe C. Dyre*

Glass and Time, IMFUFA, Department of Science and Environment, Roskilde University, P.O. Box 260, DK-4000 Roskilde, Denmark

(Dated: October 26, 2018)

Abstract

This article gives an overview of excess-entropy scaling, the 1977 discovery by Rosenfeld that entropy determines properties of liquids like viscosity, diffusion constant, and heat conductivity. We give examples from computer simulations confirming this intriguing connection between dynamics and thermodynamics, counterexamples, and experimental validations of excess-entropy scaling. Recent uses in application-related contexts are reviewed, and theories proposed for the origin of excess-entropy scaling are briefly summarized. It is shown that if two thermodynamic state points of a liquid have the same microscopic dynamics, they must have the same excess entropy. In this case, the potential-energy function exhibits a symmetry termed hidden scale invariance, stating that the ordering of the potential energies of two configurations is maintained if these are scaled uniformly to a different density. This property leads to the so-called isomorph theory, which provides a general framework for excess-entropy scaling and illuminates, in particular, why it does not apply rigorously and universally. It remains an open question whether all aspects of excess-entropy scaling and related regularities reflect hidden scale invariance in one form or other.

* dyre@ruc.dk

I. INTRODUCTION

Entropy is one of the most fascinating concepts of the physical sciences. It is deeply connected to another fundamental concept – time – because the direction of time is that of increasing entropy. In fact, the second law of thermodynamics is the only fundamental law of physics that is not time reversible. In 1977 a brief paper by Rosenfeld appeared in Physical Review entitled "Relation between the transport coefficients and the internal entropy of simple systems" [1], which proposed a relation between entropy and time with no obvious relation to irreversibility: a liquid's equilibrium dynamical properties are controlled by its entropy. Despite the intriguing nature of this claim what became known as *excess-entropy scaling*, for many years attracted little interest from the scientific community. Thus until his death in 2002, Rosenfeld's seminal paper had been cited less than twenty times, half of which were autocitations.

Rosenfeld's paper reported computer simulation results for simple model liquids of point particles like the well-known Lennard-Jones system [2]. His argument for excess-entropy scaling was based on the quasiuniversality of simple liquids that is traditionally explained by reference to the hard-sphere-system based van der Waals picture of liquids [3–5]. A possible explanation of the initial lack of interest in excess-entropy scaling is that after about 1980, the consensus in the liquid-state community was that simple liquids are well understood in terms of the hard-sphere reference system via the Weeks-Chandler-Andersen [6] and Barker-Henderson [7] perturbation theories – the focus had moved to more complex systems.

Since the onset of the new millennium there has been a steadily growing interest in excess-entropy scaling, which has turned out to apply more generally than originally thought, e.g., also for mixtures, molecular liquids, confined systems, etc. While this has highlighted the importance of the excess entropy thermodynamic variable, at the same time it has been realized that excess-entropy scaling has several exceptions and cannot be a general, rigorous consequence of statistical mechanics. In regard to the non-rigorous nature of excess-entropy scaling, Hoover already in 1986 described the situation as follows: "this scaling relationship is, like the van der Waal's equation of state, a semiquantitative model, rather than a theory" [8]. Rosenfeld confirmed this characterization in 1999, adding "like any corresponding-states relationship that links non-scaling force laws, excess-entropy scaling

can only be approximate" [9].

There is no universal link between thermodynamics and dynamics because thermodynamics reflects equilibrium probabilities of states whereas dynamics reflects the rate of transitions between the states [10]. As an illustration, consider the random barrier model of a particle jumping on a lattice with identical energies and randomly varying nearest-neighbor jump probabilities. This model has a trivial thermodynanmics, in fact zero specific heat, but a highly complex and spatially heterogenous dynamics as reflected, e.g., in the particle mean-square displacement as a function of time [11].

This Perspective article provides a brief review of excess-entropy scaling aimed at non-experts. After summarizing some necessary preliminaries in Sec. II, Sec. III presents examples of excess-entropy scaling from computer simulations. Selected experimental data are shown in Sec. IV. Section V gives examples of how excess-entropy scaling has been applied recently, e.g., for deriving viscosity models for industrial purposes. Section VI presents some of the theoretical explanations of excess-entropy scaling proposed over the years, beginning with Rosenfeld's own hard-sphere-model based justification. Section VII shows that if excess-entropy scaling is a consequence of the property that state points with the same excess entropy have the same microscopic dynamics, the system in question must conform to "hidden scale invariance". This symmetry, which states that a uniform scaling of configurations maintain the ordering of their potential energies, compare Eq. (19) below, applies to a good approximation for many liquids and solids but is never exact for realistic systems. Hidden scale invariance implies that the thermodynamic phase diagram becomes effectively one-dimensional in regard to structure and dynamics. The "isomorph theory" for the dynamics of systems that obey hidden scale invariance to a good approximation is a semi-rigorous theoretical framework, which quantifies the consequences of hidden scale invariance. Isomorph theory does not apply universally, only for systems with strong virial potential-energy correlations. On the other hand, it covers not just bulk, single-component, simple liquids, but also mixtures, molecular systems, solids, confined systems, out-of-equilibrium situations, etc. In this way the isomorph theory takes excess-entropy scaling considerably beyond Rosenfeld's original focus (Sec. VIII). Section IX gives a brief outlook.

II. PRELIMINARIES

Consider a system in thermodynamic equilibrium at temperature T with (number) density $\rho \equiv N/V$ in which N is the number of atoms or molecules ("particles") and V is the volume. The system may consist of identical particles or mixtures of two or more different types of particles. If $S(\rho, T)$ is the system's entropy, the excess entropy $S_{\rm ex}$ is defined by subtracting from S the entropy of an ideal gas at the same temperature and density, $S_{\rm id}$:

$$S_{\rm ex}(\rho, T) \equiv S(\rho, T) - S_{\rm id}(\rho, T)\,. \tag{1}$$

According to statistical mechanics entropy is the logarithm of the phase-space volume of all microscopic states consistent with the given macroscopic thermodynamic condition; thus entropy quantifies our ignorance about the system's microscopic state [10, 12]. Because the molecules of an ideal gas are "all over the place" with equal probability, the ideal-gas state corresponds to maximum ignorance or, as often stated, is maximally disordered. Consequently, $S_{\rm ex} \leq 0$ always applies. Note that $S_{\rm ex}$ increases with temperature just like the full entropy S does; in fact $S_{\rm ex} \to 0$ as temperature increases towards infinity at fixed density because the system approaches an ideal gas.

Not just the entropy, but also the Helmholtz and Gibbs free energies may be written as sums of an ideal-gas term and an excess term deriving from the interactions [5, 13]. The system energy itself, E, is a sum of the kinetic energy and the potential energy U; the latter is zero for an ideal gas so U is the excess energy. The general relation $T = (\partial E/\partial S)_\rho$ has the following analogue referring to the configurational degrees of freedom [12, 14, 15]:

$$T = \left(\frac{\partial U}{\partial S_{\rm ex}}\right)_\rho\,. \tag{2}$$

Just as entropy and free energy are sums of an ideal-gas term and a term reflecting the loss of configurational degrees of freedom due to interactions, the same is the case for their derivatives. The pressure p, for instance, is given [13] as

$$pV = Nk_BT + W \tag{3}$$

in which W is the virial, an extensive quantity of dimension energy that is zero for an ideal gas, i.e., so W/V is the excess pressure. The virial, which can be both positive and negative,

is related to the potential energy [5, 13] by

$$W = \left(\frac{\partial U}{\partial \ln \rho} \right)_{S_{\rm ex}} . \tag{4}$$

Excess-entropy scaling uses so-called macroscopically *reduced units*. In contrast to traditional unit systems, reduced units vary with the thermodynamic state point in question. The density defines the length unit l_0, the temperature defines the energy unit e_0, and the density and thermal velocity together define the time unit t_0. If m is the average particle mass, the length, energy, and time units are given [1, 8, 14] by

$$l_0 = \rho^{-1/3} \ , \ e_0 = k_B T \ , \ t_0 = \rho^{-1/3} \sqrt{m/k_B T} \, . \tag{5}$$

It may seem impractical to employ a unit system that depends on the state point. On the other hand, these units do not require knowledge of the system's Hamiltonian (the fact that the average particle mass m appears in Eq. (5) is immaterial since this is just a constant).

Quantities made dimensionless by scaling with the above units are referred to as *reduced*, which is henceforth indicated by a tilde. Consider, for instance, two quantities that Rosenfeld discussed in his original paper [1], the diffusion constant D and the viscosity η [16]. Since D has dimension length squared over time, which is formally written $[D] = l^2/t$, one defines $\tilde{D} \equiv D/(l_0^2/t_0)$, i.e.,

$$\tilde{D} \equiv \left(\rho^{1/3} \sqrt{m/k_B T} \right) \, D \, . \tag{6}$$

Viscosity is shear stress over shear rate. The former has dimension energy over volume and the latter has dimension inverse time, so $[\eta] = et/l^3 = m/(lt)$ since $[e] = ml^2/t^2$ (compare the kinetic energy expression $mv^2/2$). Thus

$$\tilde{\eta} \equiv \left(\rho^{-2/3} / \sqrt{m k_B T} \right) \, \eta \, . \tag{7}$$

This dimensionless viscosity is found already in Andrade's theory of viscosity from the 1930s [17].

We can now define: *A liquid obeys excess-entropy scaling if its reduced dynamic properties at different temperatures and pressures are determined exclusively by* $S_{\rm ex}$. In other words, the lines of constant $S_{\rm ex}$ in the thermodynamic phase diagram are lines of invariant reduced dynamics. This is the ideal situation; in practice, a system may obey excess-entropy

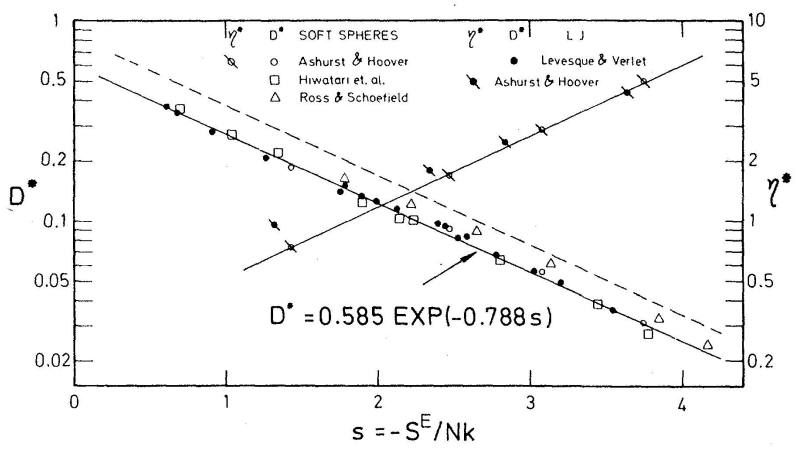

FIG. 1. Figure from Rosenfeld's seminal 1977 excess-entropy publication showing simulation data for the reduced diffusion constant (left) and the reduced viscosity (right) as a function of the negative excess entropy per particle. Data are shown for the standard Lennard-Jones (LJ) liquid and the purely repulsive "soft-sphere" inverse-power-law pair potential $v(r) \propto r^{-12}$. Rosenfeld discovered that the two systems give almost the same results for the dependence on excess entropy and, moreover, that the reduced diffusion constant and viscosity – in the figure denoted by D^* and η^* – are both approximately exponential functions of the excess entropy (Eq. (8)). Reproduced with permission from Ref. 1; copyright 1977 the American Physical Society.

scaling for some variables and not for others. For instance, one could imagine that all standard reduced transport coefficients – each of which corresponds to an integral of a time-autocorrelation functions – are functions exclusively of $S_{\rm ex}$ while, e.g., the relevant reduced time-autocorrelation function itself is not. In this paper we adopt the pragmatic point of view that excess-entropy scaling is a property that may or may not apply for the dynamics of any given reduced quantity.

Figure 1 is reproduced from Rosenfeld's original publication [1]. The x-axis is the negative excess entropy per particle. The figure shows simulation data for the reduced diffusion constant and the viscosity of the Lennard-Jones (LJ) system and a purely repulsive inverse-power-law pair-potential system. The reduced diffusion constant is shown to the left, the reduced viscosity to the right (denoted by D^* and η^*, respectively). The systems follow very similar trends. The same was reported for the one-component plasma, the system of same-charge particles interacting via Coulomb forces in a neutralizing background of opposite

charge, as well as for the hard-sphere system [1]. The diffusion data fall roughly on a line, indicating an exponential dependence on the excess entropy per particle,

$$\tilde{D} \propto e^{\alpha S_{\rm ex}/(Nk_B)} \,. \tag{8}$$

Here $\alpha \cong 0.8$ is a numerical constant. A similar expression applies for the viscosity data in Fig. 1. Such exponential dependencies on $S_{\rm ex}$ of a reduced transport coefficient is nowadays referred to as "Rosenfeld scaling". As we shall see in the next sections, many systems are known conforming to excess-entropy scaling, but not all of them obey Rosenfeld scaling.

III. SIMULATION

Much of the evidence for excess-entropy scaling comes from computer simulations. We show in this section examples of this and discuss, at the end, how lines of constant excess entropy in the thermodynamic phase diagram are identified.

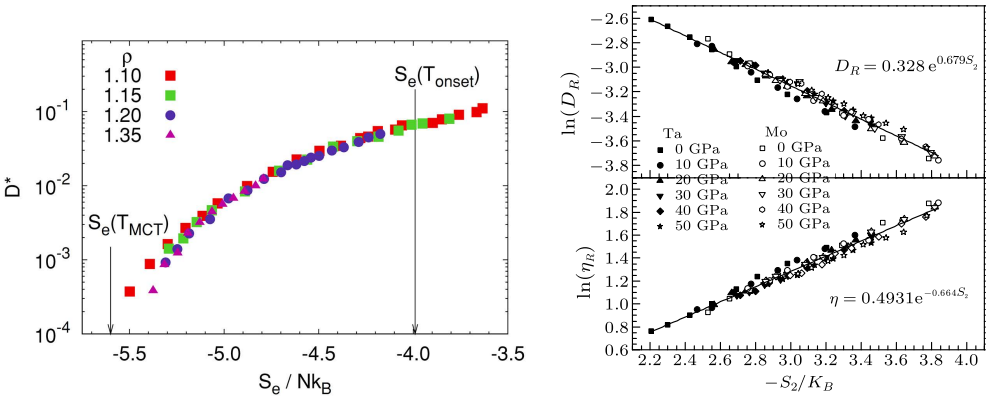

FIG. 2. Excess-entropy scaling for systems of point particles. (a) Simulations of the reduced diffusion constant of the Kob-Andersen binary Lennard-Jones model [18] at different densities and temperatures. These data conform to excess-entropy scaling, but the exponential Rosenfeld scaling Eq. (8) does not apply at low temperatures (left part of figure). Reproduced with permission from Ref. 19; copyright 2011 AIP Publishing. (b) Excess-entropy scaling of liquid tantalum and molybdenium described by many-body potentials. The excess entropy is here represented by the two-particle entropy S_2, which often provides a good estimate of $S_{\rm ex}$ (see, however, Fig. 7 below). Rosenfeld scaling works well for these data. Reproduced with permission from Ref. 20; copyright 2014 Chinese Physics Letters.

Figure 2 shows data for liquids of point particles, with (a) giving the reduced diffusion constant of the iconic Kob-Andersen binary Lennard-Jones (LJ) liquid at different temperatures and densities, a standard model in the study of viscous liquids and the glass transition [18, 21]. The data collapse nicely, demonstrating excess-entropy scaling; Rosenfeld scaling Eq. (8) does not apply accurately although it is a good approximation to the high-temperature data. Figure 2(b) shows data for two metals modeled by many-body potentials. Rosenfeld scaling applies for both metals, but note that the dynamic range is here much smaller than in Fig. 2(a). In Fig. 2(b) the excess entropy is approximated by its two-particle value S_2 (see below) [22].

Figure 3 shows simulation data for molecular models with (a) giving results for united-atom models of four hydrocarbons and (b) showing data for the symmetric dumbbell model consisting of two LJ spheres connected by a rigid bond. In both cases excess-entropy scaling works well. (b) gives data for two different inverse relaxation times. The fast one is that of the reorientation dynamics, the slow one is the decay time of periodic density fluctuations at the wave vector corresponding to the maximum of the static structure factor. Despite a difference of more than one decade, both relaxation times conform to excess entropy scaling. Rosenfeld scaling applies for all state points studied in (a), whereas in panel (b) – like in Fig. 2(a) – Rosenfeld scaling only applies at high temperatures, corresponding to low magnitudes of $S_{\rm ex}$. (c) shows data for the incoherent intermediate scattering function as a function of time for the asymmetric dumbbell model probed along a curve of constant $S_{\rm ex}$. The figure demonstrates that for this model not only the average relaxation time, but the entire dynamic signal is invariant along configurational adiabats. In experiments such an invariance is referred to as "isochronal superposition" [26]; in practice this is tested by checking whether, independent of temperature and pressure, the average relaxation time determines the entire relaxation curve [27] (compare Fig. 9 below).

A molecular model with internal degrees of freedom is considered in Fig. 4 presenting data for the flexible LJ-chain model, which consists of LJ particles connected by rigid, freely rotating bonds. Figure 4(a) shows the reduced viscosity for chain lengths 2, 4, 8, 16, while (b) shows the reduced thermal conductivity. Excess-entropy scaling applies in both cases. The viscosity is chain-length dependent, but the thermal conductivity is not. Rosenfeld scaling applies for the viscosity at low temperatures, indicated by dashed lines in (a). (c) shows data for three different intermediate scattering functions of the LJ chain model, demonstrating

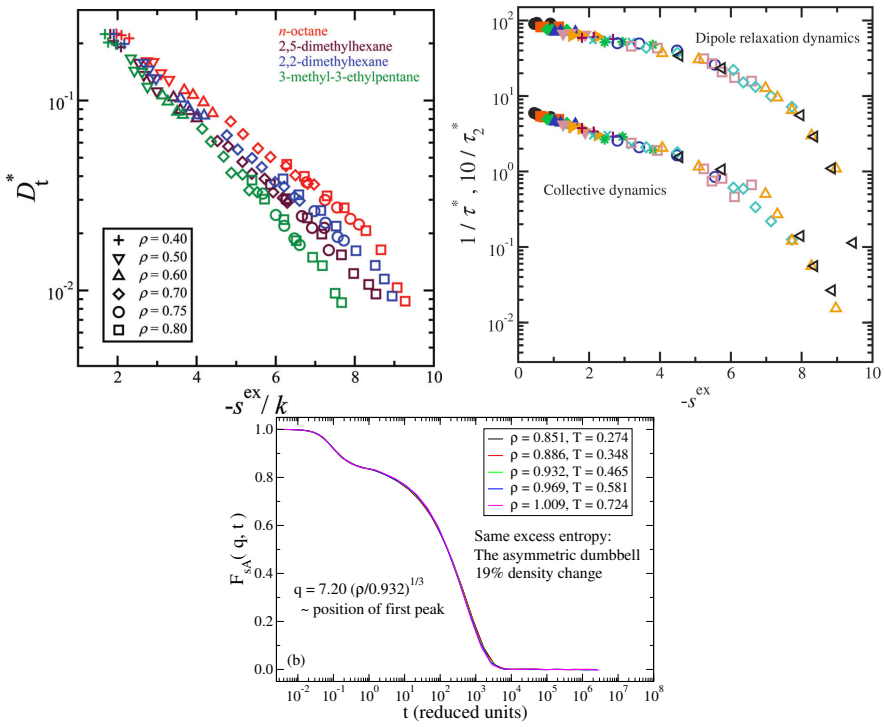

FIG. 3. Numerical data demonstrating excess-entropy scaling for molecular liquids. (a) Reduced diffusion constant at different densities of unit-atom models of n-octane, 2,5-dimethylhexane, 2,2-dimethylhexane, and 3-methyl-3-ethylpentane, all conforming to Rosenfeld scaling Eq. (8). Reproduced with permission from Ref. 23; copyright 2010 the American Chemical Society. (b) Inverse relaxation times of the coherent intermediate scattering function ("collective dynamic") and of the individual molecular reorientation dynamics for the symmetric dumbbell model consisting of two Lennard-Jones spheres connected by a rigid bond [24]. Although the two dynamics are quite different, they both conform to excess-entropy scaling. Reproduced with permission from Ref. 24; copyright 2010 AIP Publishing. (c) Incoherent intermediate scattering function for the asymmetric dumbbell model of two different LJ particles, evaluated along a curve of constant excess entropy. These data refer to highly viscous liquid state points; data along an isotherm with a smaller density variation exhibit more than three decade's change of the average relaxation time [25]. Reproduced with permission from Ref. 25.

invariant dynamics along a line of constant excess entropy, i.e., isochronal superposition. For comparison, (d) shows the same quantities along an isotherm. In all cases, Fig. 4 shows results for chain lengths that are too short to exhibit entanglement. For longer chains the picture is more complex; here excess-entropy scaling applies only if a renormalization of the

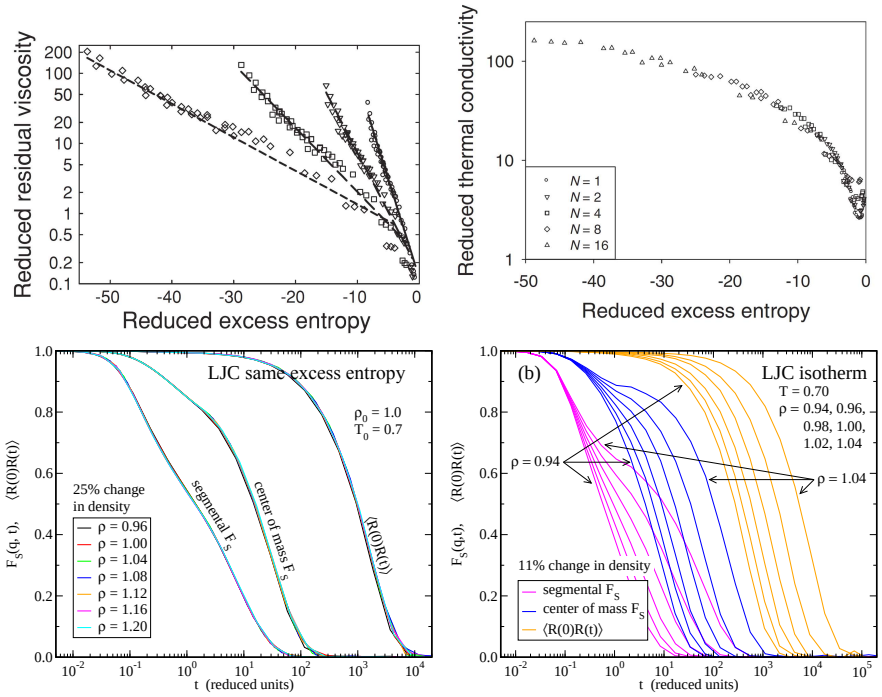

FIG. 4. Numerical data for the system of Lennard-Jones chains consisting of LJ particles connected by fixed-length freely rotating bonds, a primitive polymer model. (a) Reduced residual viscosity, i.e., subtracting the zero-density viscosity, for different chain lengths (from right to left: $2, 4, 8, 16$). Reproduced with permission from Ref. 28; copyright 2011 AIP Publishing. (b) Reduced thermal conductivity for the indicated chain lengths, showing little length dependence. Reproduced with permission from Ref. 29; copyright 2009 the American Physical Society. (c) Reduced incoherent intermediate scattering functions for seven state points with same excess entropy. Reproduced with permission from Ref. 30; copyright 2014 AIP Publishing. (d) The same quantity for seven state points at the same temperature. In (c) and (d) three different dynamics are considered for a chain-length 10 system: the dynamics of the individual segments, of the center of mass, and of the end-to-end vector. Reproduced with permission from Ref. 30; copyright 2014 AIP Publishing.

diffusion constant is allowed for [31].

Figure 5 compares data for liquids confined to small volumes to those of the corresponding bulk liquids, with (a) giving data for the hard-sphere diffusion constant. The same excess-entropy dependence applies for both the confined and bulk liquids. This striking behavior is also observed in (b), which shows relaxation-time data for the asymmetric dumbbell model in both bulk and confinement. The fact that data referring to quite different boundary

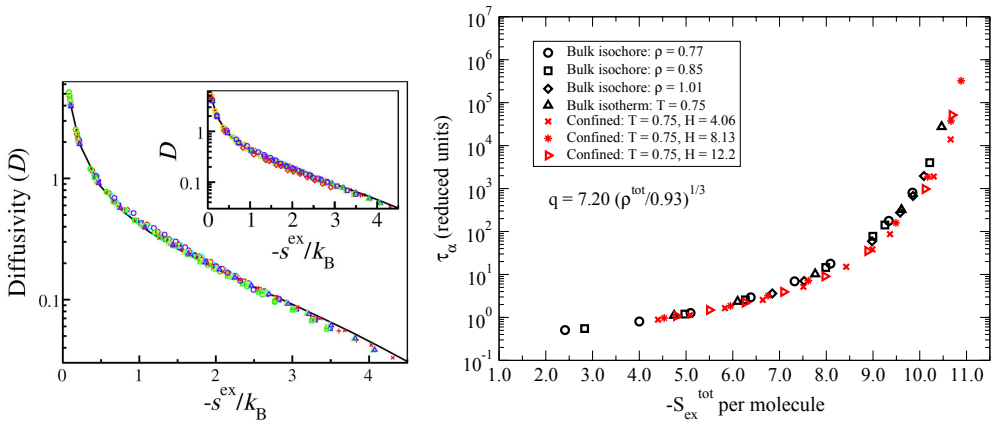

FIG. 5. Excess-entropy scaling of bulk and confined liquids. (a) Diffusion constant of hard-sphere fluids in 2d channels and in the bulk (solid curve); the symbols correspond to different confining square-well potentials. The inset includes data also for 1d channels [32]. Independent of confinement conditions, the diffusion constant is the same function of the excess entropy. Reproduced with permission from Ref. 32; copyright 2006 the American Physical Society. (b) Reduced spatially averaged structural relaxation time for the asymmetric dumbbell model plotted as a function of the excess entropy. Again, the same $S_{\rm ex}$ dependence applies for bulk- and confined-liquid data. Reproduced with permission from Ref. 33; copyright 2013 the American Physical Society.

conditions collapse as a function of the excess entropy emphasizes the fundamental role of this thermodynamic variable.

Excess-entropy scaling does not always apply [34, 36–39]. Figure 6 shows examples of this, reporting data for (a) the Hertzian model, (b) a standard water model, (c) the Stillinger-Weber potential, and (d) the Fermi-Jagla model. Liquids with anomalies like water or silica that have, e.g., a diffusion constant which increases instead of decreases upon isothermal compression or which expand upon freezing, usually disobey excess-entropy scaling in the regions of the phase diagram where the anomalies appear [35, 40–42].

How is the excess entropy determined in simulations? Chopra *et al.* [24] employed a two-step process to determine the Helmholtz free energy F by first determining F's density dependence from a grand-canonical transition-matrix Monte Carlo simulation at high temperature, subsequently using a canonical-ensemble simulation to determine the free energy's temperature variation at constant density. From F the excess entropy is easily determined. Agarwal *et al.* calculated $S_{\rm ex}$ using thermodynamic integration with an ideal-gas reference

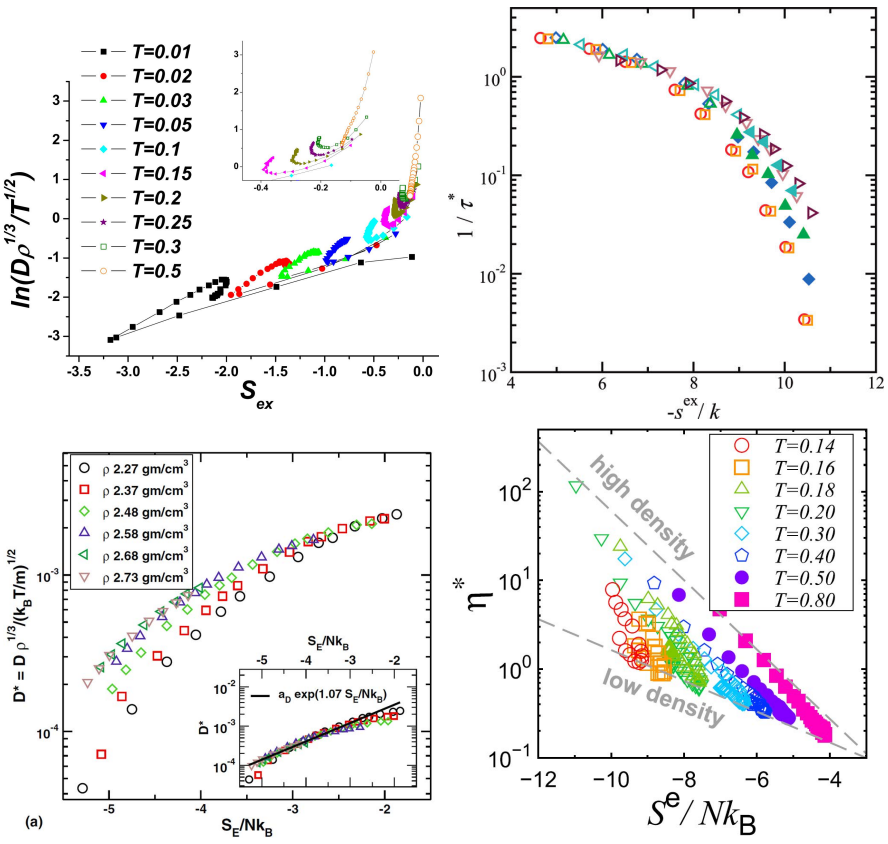

FIG. 6. Counterexamples to excess-entropy scaling. (a) Reduced diffusion constant along several isotherms for the Hertzian sphere system defined by interaction energy varying with distance as $(\sigma - r)^{5/2}$ below a cutoff at σ. The inset shows additional data from higher temperature isotherms. Reproduced with permission from Ref. 34; copyright 2010 the American Physical Society. (b) Reduced inverse collective relaxation time for the SPC/E water model. Reproduced with permission from Ref. 35; copyright 2010 the American Chemical Society. (c) Reduced diffusion constant for silicon modeled by the Stillinger-Weber potential. If a density-dependent empirical scaling is allowed for, approximate Rosenfeld scaling Eq. (8) applies (inset). Reproduced with permission from Ref. 36; copyright 2014 AIP Publishing. (d) Reduced viscosity for the Fermi-Jagla model. Reproduced with permission from Ref. 37; copyright 2018 AIP Publishing.

state [19]. Vasisht *et al.* used thermodynamic integration by first finding the excess entropy at zero pressure at a reference temperature and from this calculating $S_{\rm ex}$ for $p = 0$ at other temperatures, in the final step moving to non-zero pressure [36].

The excess entropy may be evaluated analytically if the equation of state is known [28]. Rosenfeld, for instance, for the hard-sphere reference system used the Carnahan-Starling

equation of state to calculate $S_{\rm ex}$ as a function of the hard-sphere packing fraction [1].

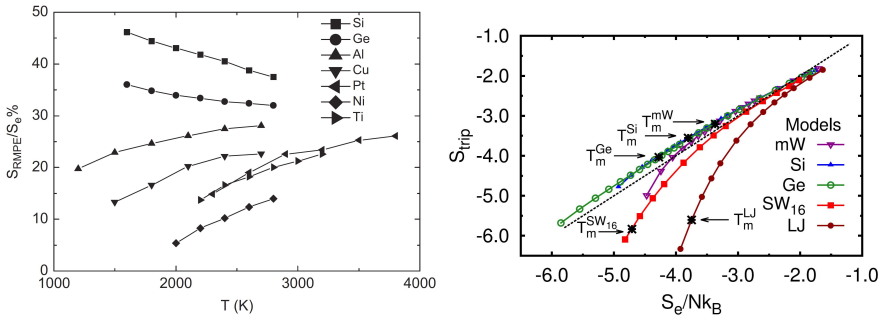

FIG. 7. Numerical data demonstrating violations of the often assumed near identities $S_{\rm ex} \cong S_2$ and $S_{\rm ex} \cong S_2 + S_3$. (a) The residual multiparticle entropy $S_{\rm RMPE} \equiv S_{\rm ex} - S_2$ relative to $S_{\rm ex}$ for melts of selected elements modeled by realistic potentials [43]. For the metals S_2 constitute at least 70% of $S_{\rm ex}$, but for silicon and germanium deviations are larger than 30%. Reproduced with permission from Ref. 43; copyright 2011 Elsevier. (b) Correlation between $S_{\rm ex}$ and S_2+S_3 for different models. In many cases $S_{\rm ex} \cong S_2 + S_3$, but for the monatomic water (mW) and Stillinger-Weber (SW) [44] models this is not a good approximation at low temperatures. Reproduced with permission from Ref. 45; copyright 2015 AIP Publishing.

A systematic expansion of $S_{\rm ex}$ exists in terms of two-particle, three-particle, etc, contributions [46, 47],

$$S_{\rm ex} = S_2 + S_3 + S_4 + \dots . \tag{9}$$

The two-particle contribution per particle is calculated from the radial distribution function $g(r)$ as follows [46, 47]

$$S_2/N = -2\pi\rho \int_0^\infty \big(g(r)\ln g(r) - g(r) + 1\big) r^2 dr \,. \tag{10}$$

In many cases this gives the dominant contribution to $S_{\rm ex}$ [47]. This is fortunate because $g(r)$ is a standard outcome of simulations. It is not generally the case, however, that $S_{\rm ex} \cong S_2$ [48–53]. Examples where this identity does not work well are given in Fig. 7.

If one is primarily interested in *whether or not* excess-entropy scaling applies, more than in *how* different reduced quantities vary with $S_{\rm ex}$, the lines of constant $S_{\rm ex}$ in the thermodynamic phase diagram are conveniently identified without knowledge of $S_{\rm ex}$ by means of the following statistical-mechanical fluctuation identity [14]

$$\left(\frac{\partial \ln T}{\partial \ln \rho}\right)_{S_{\rm ex}} = \frac{\langle \Delta U \Delta W \rangle}{\langle (\Delta U)^2 \rangle}\,. \tag{11}$$

Here, the angular brackets denote NVT canonical thermal averages at the state point in question and Δ refers to the given quantity minus its state-point average. If, for instance, the right-hand side is 3, a one percent increase of density is to be accompanied by a 3% increase of temperature in order to keep $S_{\rm ex}$ constant. Recalculating the right-hand side at the new state point allows for step-by-step mapping out a line of constant excess entropy in the phase diagram [14].

IV. EXPERIMENT

Figure 8 shows experimental data for the viscosity and diffusion constant measured at various pressures and temperatures. The first three figures report the reduced viscosity of argon, carbon dioxide, and methane, as a function of the excess entropy ("reduced residual entropy"). These data are from experiments by Abramson measuring the viscosity over a large range of temperatures and pressures up to 6-8 GPa, using a rolling-ball technique. (d) and (e) give the diffusion constant of alkanes and a colloidal monolayer, respectively, as a function of the excess entropy.

Identifying $S_{\rm ex}$ in experiments is not straightforward. We refer to the references of Fig. 8 for details. In practice, the determination of $S_{\rm ex}$ at a given state point is often based on the use of an equation of state, e.g., expressed via the Helmholtz free energy as a function of temperature and density, fitted to the thermodynamic data [55, 60, 61]. If one assumes the system in question obeys excess-entropy scaling for all dynamic processes, the dynamics measured on a certain time scale may be used to identify the lines of constant $S_{\rm ex}$. This leads to the above-mentioned principle of isochronal superposition [26, 27], according to which two state points with the same average reduced relaxation time have the same relaxation spectra. As shown in Sec. VII, if two state points have the same microscopic dynamics (except for a uniform scaling of space and time), they must have the same $S_{\rm ex}$. Figure 3(c) and Fig. 4(c) showed instances of isochronal superposition in computer simulations. Experimental examples are given in Fig. 9 in which (a) shows how dielectric spectra at different temperatures and pressures superpose if the loss-peak frequency is the same. An example of isochronal superposition over fourteen orders of magnitude was recently given by Hansen *et*

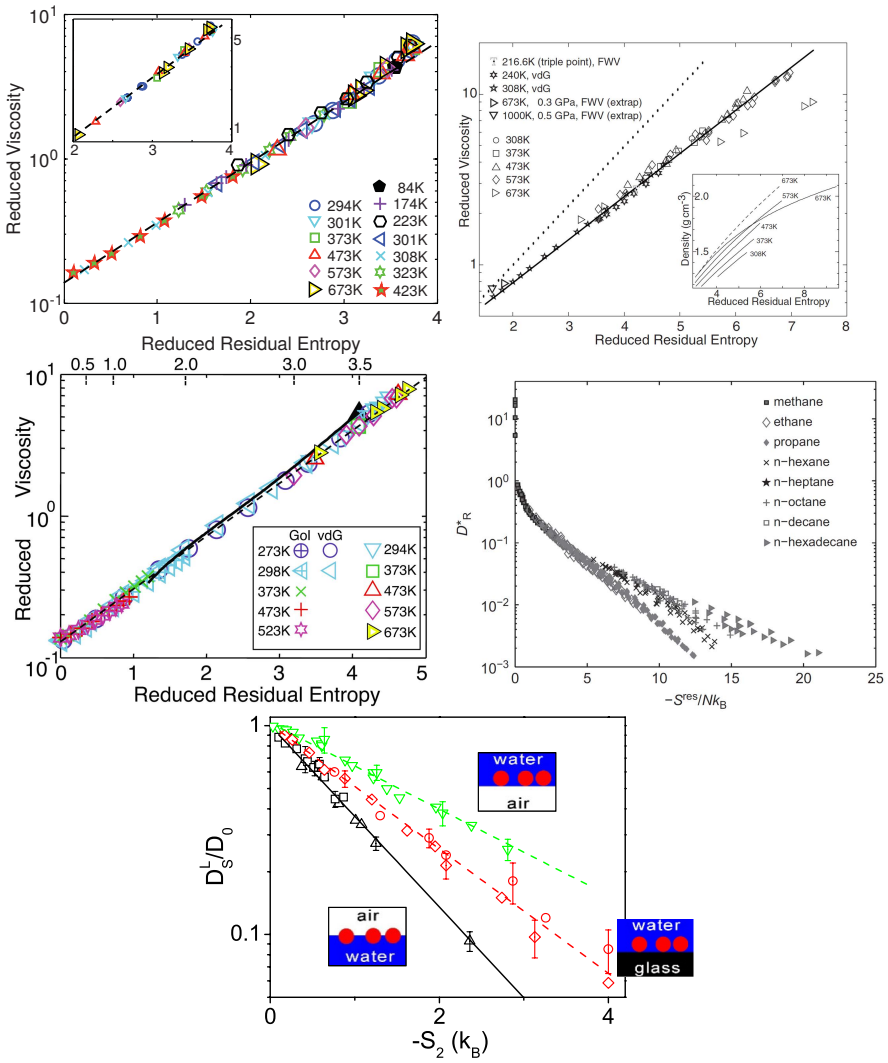

FIG. 8. Experimental viscosity data demonstrating excess-entropy scaling. The first three figures show data for the following fluids: (a) Argon. Reproduced with permission from Ref. 54; copyright 2011 Taylor & Francis Ltd. (b) Carbon dioxide. Reproduced with permission from Ref. 55; copyright 2009 the American Physical Society. (c) Methane. Reproduced with permission from Ref. 56; copyright 2011 the American Physical Society. In (a), (b), and (c) the reduced viscosity is a function of the excess entropy, referred to as "reduced residual entropy". (d) shows diffusion-constant data for n-alkanes. Reproduced with permission from Ref. 57; copyright 2012 Elsevier. (e) shows data for a colloidal monolayer. Reproduced with permission from Ref. 58; copyright 2013 the American Physical Society.

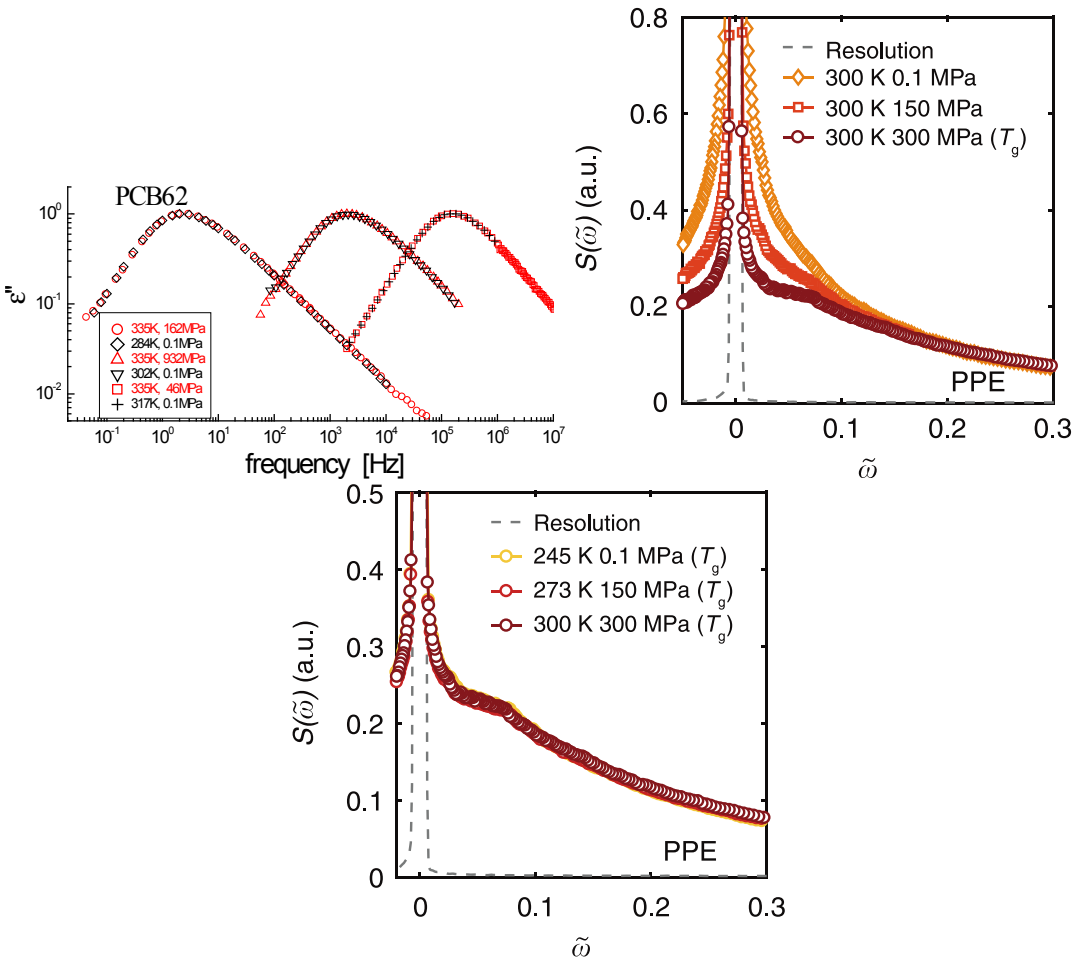

FIG. 9. Isochronal superposition in experiments. Lines of constant excess entropy in the thermodynamic phase diagram are identified from the invariance of a selected dynamic characteristic. Isochronal superposition predicts invariance of all dynamic characteristics along these lines. (a) Dielectric loss data at different temperatures and pressures for the chlorinated biphenyl PCB62. When loss-peak frequencies are identical, the entire spectra overlap. Reproduced with permission from Ref. 27; copyright 2005 the American Chemical Society. (b) and (c) show the dynamics of 5-polyphenyl-ether (PPE) probed on the picosecond time scale by inelastic time-of-flight neutron scattering experiments. (b) shows spectra at 300K at three different pressures, while (c) shows spectra at three different state points along the glass-transition isochrone, i.e., with the same slow dynamics. The overlap in (c) demonstrates isochronal superposition over fourteen decades in time. (b) and (c) are reproduced with permission from Ref. 59.

al. [59]. For two van der Waals liquids, it was shown that state points with different temperature and pressure but same relaxation time on the second time scale (probed by dielectric spectroscopy) have the same dynamics on the picosecond time scale (probed by neutron scattering). Isochronal data for one of these liquids are shown in Fig. 9(c), which may be compared to isothermal data shown in Fig. 9(b). Interestingly, isochronal superposition does not apply for a hydrogen-bonded liquid studied with the same techniques [59].

V. APPLICATION

Highly relevant for industrial applications, excess entropy has recently been identified as the crucial quantity for rationalizing, e.g., how the bulk or confined-geometry viscosity and diffusion constant vary throughout the thermodynamic phase diagram [61–67]. Excess-entropy-scaling based models have been applied to transport properties of electrolytes and silica melts [68, 69], methane and hydrogen absorption in metal-organic frameworks [70, 71], the viscosity and thermal conductivity of refrigerants and other liquids [72, 73], the viscosity of the Earth's iron-nickel liquid core at the relevant extreme pressures [74], separation of carbon isotopes in methane with nanoporous materials [75, 76], etc. As stated by Novak, models based on the excess entropy provides a "practical approach to determining viscosity in process engineering, product engineering, oil and gas reservoir engineering, pipelines, and fracking applications" [77]. A more basic-research oriented use of excess-entropy scaling was recently reported in a paper on understanding water structure and dynamics in protein hydration layers [78].

Figure 10 gives examples of how experimental data in application-relevant contexts are rationalized, either by use of the excess entropy itself or by models based on it, usually with one or more fitting parameters. (a) shows data for methane diffusion in zeolites and (b) shows data for bulk n-alkane viscosity. (c) shows ketone data versus excess entropy calculated from the so-called perturbed-chain statistical associating fluid theory (PCP-SAFT) [81], while (d) shows isopropyl-benzene's reduced thermal conductivity versus its excess entropy.

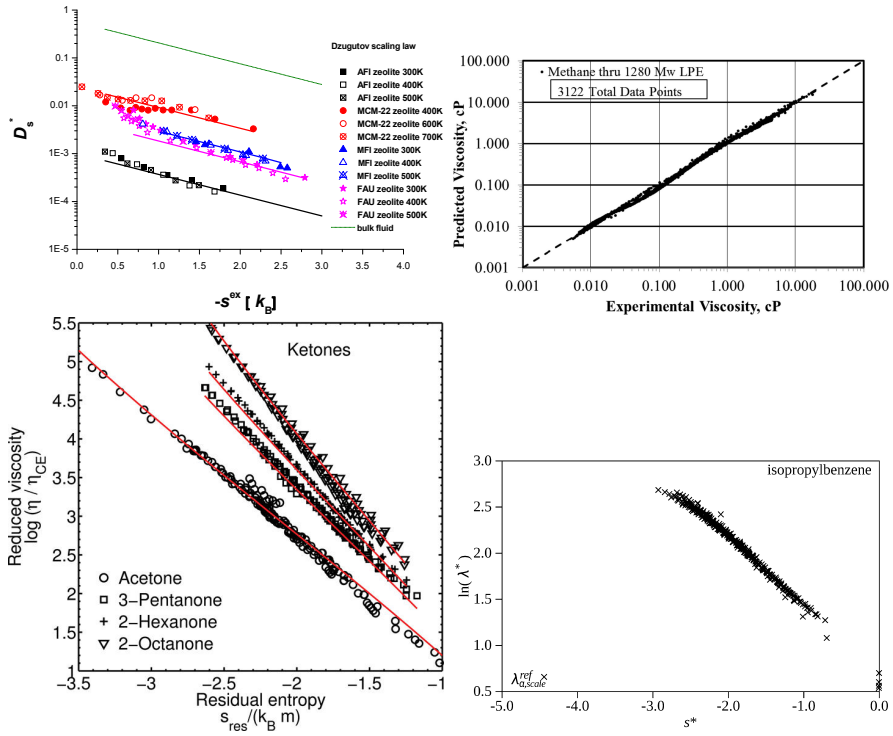

FIG. 10. Data relevant for industrial applications rationalized via the excess entropy. (a) Reduced diffusion constant of methane in zeolites versus the negative excess entropy per particle, demonstrating excess-entropy scaling. Reproduced with permission from Ref. 79; copyright 2014 Elsevier. (b) Predictions of an "entity-based" scaled viscosity model versus data over the entire fluid region for seventeen n-alkanes, ranging from methane to molecular-weight 1280 g/mol linear polyethylene. Reproduced with permission from Ref. 77; copyright 2013 the American Chemical Society. (c) Reduced viscosity data for ketones versus residual entropies calculated from the PCP-SAFT equation of state. Reproduced with permission from Ref. 80; copyright 2015 the American Chemical Society. (d) Reduced thermal conductivity versus excess entropy of isopropyl-benzene using also this equation of state. Reproduced with permission from Ref. 73; copyright 2017 the American Chemical Society.

VI. THEORY

Since excess-entropy scaling is only approximate and does not apply universally (Fig. 6), it clearly cannot be rigorously derived for systems in general. Some of the arguments for excess-entropy scaling that have been given over the years are summarized below.

First, however, we note that there is one particular case for which excess-entropy scaling

is exact. This happens if the potential-energy function is Euler homogeneous, i.e., obeys the following requirement in which λ is a uniform scaling parameter

$$U(\lambda \mathbf{R}) = \lambda^{-n} U(\mathbf{R})\,. \tag{12}$$

In this case, the reduced-unit microscopic dynamics is rigorously invariant along the lines in the thermodynamic phase diagram defined by $\rho^{n/3}/T$ =Const [82, 83]. Physically, this reflects the fact that a change of density can be compensated entirely by a change of temperature. Since the dynamics is invariant along the $\rho^{n/3}/T$ = Const lines except for a uniform scaling of space and time, this is the case also for the excess entropy that basically measures the available reduced volume in configuration space [15, 84]. Accordingly, the lines of constant excess entropy are exact lines of invariant reduced dynamics, which implies that, e.g., $\tilde{D}$ and $\tilde{\eta}$ are unique functions of the excess entropy whenever the potential-energy function is Euler homogeneous. An often studied example is that particles interacting via purely repulsive inverse-power-law pair potentials [41, 82, 85–87].

A. Rosenfeld-Hoover-Dzugutov hard-sphere argument

The first justifications of excess-entropy scaling came from three authors giving closely related arguments based on the hard-sphere (HS) reference system. In Rosenfeld's original publication [1] the reasoning was basically as follows. If a simple liquid is well represented by a HS system, its excess entropy is equal to that of the corresponding HS liquid, which is determined by the packing ratio ϕ (the occupied fraction of space). If the excess entropy per particle is denoted by $s_{\rm ex} \equiv S_{\rm ex}/N$, this implies that $s_{\rm ex} = s_{\rm ex}(\phi)$. Assuming the HS representation applies also for dynamic properties, one has $\tilde{D} = \tilde{D}(\phi)$, which by elimination implies $\tilde{D} = \tilde{D}(s_{\rm ex})$. The new idea of Ref. 1 was that one can avoid the tricky issue of determining the effective HS packing fraction of the system at the state point in question by referring instead to a thermodynamic property that is in a one-to-one relation with ϕ, namely the excess entropy [88]. At the time, Rosenfeld did not thoroughly justify the use of macroscopically reduced units (Eq. (5)), but in 1999 he stated that these are suggested "by elementary kinetic theory for a dense medium of particles with thermal velocities but with a mean free path between collisions which is of the order of the average interparticle distance".

An important finding in Rosenfeld's 1977 paper was that the function $\tilde{D}(s_{\rm ex})$ is quasiuniversal. In particular, virtually the same function applies for systems of purely repulsive pair forces and for the Lennard-Jones system, which is highly nontrivial. From simulation data Rosenfeld found that Eq. (8) applies; similarly he found for the viscosity that $\tilde{\eta} \propto \exp(-\beta s_{\rm ex}/k_B)$ in which β like α of Eq. (8) is a numerical constant of order unity (Fig. 1). This exponential Rosenfeld scaling, which is now known not to work in all cases of excess-entropy scaling, compare the above figures, was derived in 1986 by Hoover using an effective Einstein-model for the HS system's "cage rattling" particles [8], arguing as follows: If ω_0 is the effective Einstein vibration frequency, i.e., the inverse of the time between collisions, any diffusion constant is estimated by $D \sim l_0^2\,\omega_0$ in which $l_0 = \rho^{-1/3}$ is the average interparticle distance. This applies to the heat diffusion constant, the particle diffusion constant, and the transverse momentum diffusion constant, the so-called kinematic viscosity. According to the Navier-Stokes equation, the latter is $\eta/(m\rho)$ [89], i.e., one has $\eta/(m\rho) = l_0^2\,\omega_0$. In terms of the vibrational mean-square displacement $\langle x^2\rangle$, the excess entropy per particle is the logarithm of the available space relative to the interparticle distance, $s_{\rm ex} = k_B \ln(\sqrt{\langle x^2\rangle}/l_0)$ [10, 12]. Writing the single-particle effective potential as $(1/2)m\omega_0^2 x^2$, equipartition implies $m\omega_0^2\langle x^2\rangle = k_B T$. Eliminating $\langle x^2\rangle$ leads to $\exp(s_{\rm ex}/k_B) = l_0^{-1}\omega_0^{-1}\sqrt{k_B T/m}$ or $\omega_0 = l_0^{-1}\sqrt{k_B T/m}\exp(-s_{\rm ex}/k_B)$. Combining this with $\eta/m\rho = l_0^2\,\omega_0$ leads to $\eta = m\rho l_0^2\omega_0 = \rho^{2/3}\sqrt{mk_B T}\exp(-s_{\rm ex}/k_B)$, which in reduced units (compare Eq. (7)) is simply $\tilde{\eta} = \exp(-s_{\rm ex}/k_B)$.

Unaware of Rosenfeld's at the time little known paper, Dzugutov in 1996 rediscovered excess-entropy scaling [48]. He did not use macroscopically reduced units, but scaled instead length by the effective hard-sphere radius and time by the inverse Einstein frequency. Nevertheless, Dzugutov's physical ideas and arguments are quite similar to those of Rosenfeld and Hoover. Dzugutov justified the exponential excess-entropy dependence of the transport coefficients he found from simulations as follows: "The frequency of local structural relaxations, which defines the rate of the cage diffusion, is obviously proportional to the number of accessible configurations (per atom)," which by definition of the entropy is given by $\exp(s_{\rm ex}/k_B)$. This argument leads to Rosenfeld scaling Eq. (8) with $\alpha = 1$. Dzugutov argued, moreover, that the most important contribution to $s_{\rm ex}$ is the two-particle entropy, making it possible to estimate diffusion constants from radial-distribution-function data [90].

B. Excess-entropy scaling for gasses

By reference to Enskog theory [91] and a second-order virial expansion, Rosenfeld in 1999 showed that excess-entropy scaling applies also for dilute gases of particles interacting via inverse power-law repulsive potentials, $v(r) \propto r^{-n}$. For exponents $n > 3$ the reduced viscosity, the reduced diffusion constant, and the reduced thermal conductivity all vary with excess entropy per particle in proportion to $s_{\mathrm{ex}}^{-2/3}$. This extends excess-entropy scaling to the gas phase, although Rosenfeld scaling Eq. (8) clearly does not apply in this part of phase space.

C. Kolmogorov-Sinai entropy connection

The dynamics of the hard-sphere system is determined by the rate at which trajectories in the multidimensional phase space diverges from one another in the coarse of time [92]. This rate is quantified by the so-called Kolmogorov-Sinai (KS) entropy defined as the sum of all positive Lyapunov exponents [92–94]. In 1998 an interesting connection to excess-entropy scaling was proposed by Dzugutov and coworkers in a paper demonstrating a linear relation between the KS entropy and the excess entropy for simple liquids [95]. The existence of a universal relation between diffusion constant and KS entropy for simple liquids was confirmed in 2000 in simulations by Pang and coworkers [96], as well as in a theoretical study by Samanta *et al.* in 2004; the latter paper's argument includes also the case of mixtures [97, 98].

D. Mode-coupling theory

The main postulate of mode-coupling theory is that structure determines dynamics [99]. In its simplest version, the pair distribution function $g(r)$ determines the liquid's incoherent intermediate scattering function. On the other hand, $g(r)$ also determines the two-particle contribution to the excess entropy S_2 (Eq. (10)), which as we have seen is often the dominant contribution to S_{ex}. Thus it makes good sense that mode-coupling theory predicts excess-entropy scaling in the $S_{\mathrm{ex}} \cong S_2$ approximation [53, 97, 100, 101].

E. Generalized excess-entropy scaling

Truskett and coworkers in 2009 addressed the challenge that systems with soft pair potentials generally tend to disobey excess-entropy scaling. To remedy this, they proposed a modified scaling of the diffusion constant that by construction ensures excess-entropy scaling in the low-density (gas) limit. This is done by scaling D with the product of $D\rho$ (at a reference density) and $B(1 + d\ln B/d\ln T)$, in which B is the second virial coefficient [102]. In the dilute limit, rigorous theory implies that the diffusion coefficient scaled in this way varies as $1/s_{\mathrm{ex}}$ [102]. For binary hard-sphere mixtures, Widom-Rowlinson mixtures, the Gaussian core model [103], and Hertzian particle fluids, this alternative form of excess-entropy scaling collapses diffusion-constant data much better than regular excess-entropy scaling, also in the non-dilute phase [104]. The novel scaling is not consistent with standard Rosenfeld scaling, however, so for any given system these two ways of scaling cannot both collapse dynamic quantities as a function of the excess entropy.

F. Diffusion in a rugged potential-energy landscape

The potential-energy landscape of a liquid is very complex [105]. Representing complexity by randomness [106], liquid dynamics has been modeled as jumps in a random landscape [107–109], for instance with energies distributed according to a Gaussian [110–113]. For this model Bagchi and coworkers in 2014 and 2015 showed via the effective-medium approximation that at moderate disorder, the diffusion constant is given by the Rosenfeld relation Eq. (8) with $\alpha = 1$ [114, 115].

Excess-entropy scaling applies also in the "extreme disorder limit" [11] of the Gaussian random landscape model, the limit in which barriers are much larger than k_BT and where diffusion is, consequently, controlled by percolation [112]. To see this, consider a system in d dimensions with a Gaussian density of states $n(E) \propto \exp(-E^2/2\sigma^2)$. At temperature T the energy probability distribution is given by $P(E) \propto n(E)\exp(-E/k_BT) \propto \exp(-(E - \bar{E})^2/2\sigma^2)$ in which $\bar{E}(T) = -\sigma^2/k_BT$ is the average energy. If the percolation energy is denoted by E_c, the effective barrier for escaping entirely from a state of low energy E is given by $\Delta E = E_c - E$ [112]. At low temperatures, the relevant energies move far into the negative tail of the Gaussian and one has $\Delta E \cong -E$. The diffusion constant is estimated

by $D \sim \langle l \rangle^2/\langle \tau \rangle$ in which $\langle l \rangle$ is the average distance between the most likely states and the relaxation time τ is given by $\tau = \tau_0 \exp(\Delta E/k_B T) \sim \tau_0 \exp(-E/k_B T)$ where τ_0 is a prefactor. We estimate $\langle l \rangle$ from $\langle l \rangle^{-d} \sim n(\bar{E}(T))$ leading to $\langle l \rangle \sim \exp(\bar{E}(T)^2/(2d\sigma^2))$. After evaluating a Gaussian integral one finds $\langle \tau \rangle \sim \exp(3\sigma^2/(2(k_B T)^2))$. In terms of $\bar{E}(T)$, the excess entropy is given by $S_{\rm ex}/k_B \sim \ln n(\bar{E}(T)) = -\bar{E}^2(T)/2\sigma^2 = -\sigma^2/(2(k_B T)^2)$. Combining these equations leads to $\tilde{D} \sim \exp(\alpha S_{\rm ex}/k_B)$, i.e., Rosenfeld scaling with $\alpha = 3 - 2/d$.

G. Other theoretical connections

This section discusses briefly a number of interesting works in which entropy is related to dynamics in various ways without specifically aiming at deriving excess-entropy scaling.

1. The Adam-Gibbs configurational entropy expression

In the study of glass-forming liquids, going back in time more than half a century there have been proposals of a link between the relaxation time and the "configurational entropy" defined as the entropy relative to a perfect crystalline state, just as the definition of $S_{\rm ex}$ refers to the gas state [116–118]. In fact, ever since the works of Simon [119] and Kauzmann [120] from 1931 and 1948, respectively, it has been noted that the rapid increase in structural relaxation times of liquids cooled toward their glass transition correlate with a significant drop in entropy. Martinez and Angell in 2001 reviewed the parallelism between the dramatic temperature dependence of the viscosity/relaxation time of supercooled liquids and the configurational entropy's temperature dependence [121]. More recently, a generalized entropy theory of glass formation has been proposed [122, 123], which combines the Adam-Gibbs model [118] with the so-called lattice cluster theory.

2. Relating to the geometry of the potential-energy-landscape

Chakraborty and Chakravarty have shown numerically for the Lennard-Jones system that the diffusion constant depends linearly on a number of properties characterizing the potential-energy landscape, e.g., the fraction of negative curvature directions, and mean,

maximum, and minimum eigenvalues of the Hessian matrix [124]. Assuming Rosenfeld scaling Eq. (8), this implies that the logarithm of the excess entropy exhibits the same linear dependencies, providing useful connections between the excess entropy and landscape properties.

3. Coarse-graining with the relative entropy

Scott Shell has shown that the optimal approximation to a given system by one from a specified class of simpler systems [125] is obtained by minimizing the so-called relative entropy, an information-theoretic quantity also known as the Kullback-Leibler divergence, which measures the information lost upon coarse graining [126]. Shell's "relative-entropy coarse-graining method" was designed for reducing the number of degrees of freedom, i.e., for proper coarse-graining [127], but it has also been used to approximate the Lennard-Jones system by a system with inverse power-law pair interactions [127]. In the latter case, since the relative entropy is the difference between the two systems' excess entropies, assuming Rosenfeld scaling Eq. (8) one concludes that the smaller the relative entropy is, the better does the coarse-graining approximation work for dynamic properties.

4. String-theory-based lower bound on viscosity

A surprising connection between entropy and viscosity appeared in a paper in 2005 by Kovtun *et al.*, which showed that for a large class of strongly interacting quantum field theories whose dual description involves black holes in anti-de Sitter space, the ratio of viscosity over entropy density is $\hbar/(4\pi k_B)$ [128]. The paper conjectured that this number provides a lower bound to the entropy density $\eta/(s\rho)$ where s is the entropy per particle (the excess entropy plus the ideal-gas entropy), i.e., that

$$\frac{\eta}{s\,\rho} \geq \frac{\hbar}{4\pi k_B} \cong 6 \cdot 10^{-13}\,\mathrm{Ks}\,. \tag{13}$$

This lower-bound prediction, which obviously excludes superfluids for which $\eta = 0$, has been applied to strongly interacting systems like the quark-gluon plasma created in a heavy ion collision [128] and to the electron fluid of cuprate strange metals [129]. Equation (13) is obeyed by helium and other rare gasses, as well as by water, nitrogen, ammonia, and molten

alkali metals [128, 130–132]. For these more mundane systems $\eta/(s\rho)$ reaches its minimum close to the critical point, where it is 10-100 times larger than the string-theory based lower limit Eq. (13) [132].

5. Rationalizing the behavior of anomalous systems

It is well known that water exhibits a multitude of anomalies, e.g., by having a diffusion constant that increases instead of decreases upon isothermal compression. Such anomalies are common for tetrahedrally coordinated systems and have also been reported, e.g., for the Gaussian-core model of spherically symmetric interactions based on a Gaussian function [103]. Interestingly, the anomalies correlate with entropy anomalies [35, 51, 133, 134]. Thus regions of anomalous diffusivity and density behavior appear as "nested domes" in the thermodynamic phase diagram within a structurally anomalous envelope [51]. Despite the fact that water models do not obey excess-entropy scaling, a given property exhibits anomalous behavior when the strength of the excess entropy anomaly exceeds a property-specific threshold [51].

6. Excess-entropy scaling in out-of-equilibrium situations

The excess entropy is an equilibrium thermodynamic quantity. In order to extend excess-entropy scaling to out-of-equilibrium situations, Krekelberg *et al.* proposed using the two-body excess entropy S_2 of Eq. (10) [135, 136]. The point is that S_2 is given by the radial distribution function $g(r)$, which is defined also in, e.g., a steady-state flow. This idea was applied very recently by Ingebrigtsen and Tanaka to successfully collapse relaxation time data for different systems with shear rates extending far into the nonlinear regime, in a version in which the anisotropic structure under shear was taken into account in the definition of S_2 [137].

VII. HIDDEN SCALE INVARIANCE

Rosenfeld's 1977 paper [1] reported that state points with different density and temperature but same $S_{\rm ex}$ have the same reduced diffusion constant, viscosity, and thermal

conductivity. The simplest explanation is that at state points with the same excess entropy, the system's atoms or molecules move about each other *in the same way* (to a good approximation), as suggested by the observation of isochronal superposition in Fig. 3(c) and Fig. 4(c). This section investigates the possibility that the equation of motion is approximately invariant along configurational adiabats.

If one imagines filming a liquid's particles, the same movie cannot be seen at state points with different densities. The best one can hope for is that the particle motions are identical at two state points with same $S_{\rm ex}$ *except for a uniform scaling of space and time*. To eliminate the density dependence, coordinates must be scaled by the density ρ as in the units defined in Eq. (5), compare the definition of the reduced coordinate vector $\tilde{\mathbf{R}} \equiv \mathbf{R}/l_0 = \rho^{1/3}\mathbf{R}$. Likewise, time must be scaled to ensure invariant thermal velocities along the lines of constant $S_{\rm ex}$, and this is precisely what is obtained by using the reduced time coordinate $\tilde{t}$ defined via Eq. (5).

Assuming a system of identical particles, if $\tilde{\mathbf{F}} \equiv l_0\mathbf{F}/e_0 = \rho^{-1/3}\mathbf{F}/k_BT$ is the reduced $3N$-dimensional vector of all particle forces, it is straightforward to show that Newton's equation of motion in reduced coordinates is

$$\frac{d^2\tilde{\mathbf{R}}}{d\tilde{t}^2} = \tilde{\mathbf{F}}\,. \tag{14}$$

No mass appears on the left-hand side because the particle mass is absorbed into the reduced time, compare Eq. (5). Equation (14) refers to the case of a single-component system, but all arguments given below apply also for mixtures; for a mixture the left-hand side of Eq. (14) is for each particle $(m_i/\langle m\rangle)d^2\tilde{\mathbf{r}}_i/d\tilde{t}^2 = \tilde{\mathbf{F}}_i$, but this complication does not affect the arguments given below.

Equation (14) applies for any system in equilibrium at a specified state point, whether or not the system obeys excess-entropy scaling. In general, the reduced force vector $\tilde{\mathbf{F}}$ depends on the coordinate vector $\mathbf{R}$, not just on $\tilde{\mathbf{R}}$, and the reduced dynamics at different state points are not identical. If, however, the reduced force depends only on the *reduced* coordinates, i.e., if $\tilde{\mathbf{F}} = \tilde{\mathbf{F}}(\tilde{\mathbf{R}})$, there is invariance because in this case the equation of motion has no reference to the density ρ.

How to check whether a given system obeys this requirement to a good approximation? To answer this question it is convenient to define the following microscopic excess-entropy function $S_{\rm ex}(\mathbf{R})$ [84]:

$$S_{\rm ex}(\mathbf{R}) \equiv S_{\rm ex}(\rho, U(\mathbf{R}))\,. \tag{15}$$

On the right-hand side $S_{\rm ex}(\rho, U)$ is the excess entropy of the thermodynamic state point with density ρ and average potential energy U. In words, Eq. (15) defines the excess entropy of the configuration $\mathbf{R}$ as the excess entropy of the thermodynamic state point with *average* potential energy equal to $U(\mathbf{R})$ and density corresponding to $\mathbf{R}$. The thermodynamic excess entropy of a given state point is the average of its microscopic excess entropies, i.e., $S_{\rm ex} = \langle S_{\rm ex}(\mathbf{R})\rangle$, just as the thermodynamic pressure is the average of the microscopic pressures.

The above is completely general and so is the inverse of Eq. (15),

$$U(\mathbf{R}) = U(\rho, S_{\rm ex}(\mathbf{R}))\,. \tag{16}$$

Recalling the expression for temperature Eq. (2), Eq. (16) implies for the force vector $\mathbf{F} = -\nabla U(\mathbf{R}) = -T\,\nabla S_{\rm ex}(\mathbf{R})$. The reduced force vector is given by $\tilde{\mathbf{F}} = \rho^{-1/3}\mathbf{F}/k_BT = -\tilde{\nabla} S_{\rm ex}(\mathbf{R})/k_B$ in which $\tilde{\nabla} = \rho^{-1/3}\nabla$ is the gradient operator with respect to the reduced coordinates. If $\tilde{\mathbf{F}} = -\tilde{\nabla} S_{\rm ex}(\mathbf{R})/k_B$ depends only on the reduced coordinate vector $\tilde{\mathbf{R}}$, $S_{\rm ex}(\mathbf{R})$ is a function of $\tilde{\mathbf{R}}$ plus some function of the system's overall density ρ, denoted by $\psi(\rho)$. Letting T go to infinity at fixed ρ takes the system to the gas limit in which $S_{\rm ex} \to 0$. Thus $\psi(\rho)$ is independent of ρ and may be put to zero without loss of generality. In summary, if λ is a uniform scaling factor, the "same-movie requirement" $\tilde{\mathbf{F}} = \tilde{\mathbf{F}}(\tilde{\mathbf{R}})$ implies

$$S_{\rm ex}(\mathbf{R}) = S_{\rm ex}(\lambda\mathbf{R})\,. \tag{17}$$

This scale-invariance condition demonstrates, once again, the importance of the excess entropy. In particular, it follows that the only possible lines of invariant microscopic dynamics in the phase diagram are the configurational adiabats, the lines of constant $S_{\rm ex}$. This is not surprising, given the fact that the excess entropy is basically the logarithm of the reduced volume traced out in the course of time [10, 12].

Since $S_{\rm ex}$ for a system with hidden scale invariance depends only on a configuration's reduced coordinates $\tilde{\mathbf{R}}$, Eq. (16) becomes

$$U(\mathbf{R}) = U(\rho, S_{\rm ex}(\tilde{\mathbf{R}}))\,. \tag{18}$$

How does one test whether Eq. (17) or, equivalently Eq. (18), applies to a good approximation for a given system? Consider two arbitrary configurations corresponding to the same density, $\mathbf{R}_{\rm a}$ and $\mathbf{R}_{\rm b}$, and suppose that $U(\mathbf{R}_{\rm a}) < U(\mathbf{R}_{\rm b})$. Since $(\partial U/\partial S_{\rm ex})_\rho = T > 0$, one concludes from Eq. (18) that $S_{\rm ex}(\tilde{\mathbf{R}}_{\rm a}) < S_{\rm ex}(\tilde{\mathbf{R}}_{\rm b})$. Equation (18) then implies that a uniform scaling of the two configurations to a different density preserves the relation between their potential energies. That is, if one configuration has lower potential energy than another, this is the case also after a uniform scaling. Formally, this property is expressed in the following logical implication [84]:

$$U(\mathbf{R}_{\rm a}) < U(\mathbf{R}_{\rm b}) \Rightarrow U(\lambda\mathbf{R}_{\rm a}) < U(\lambda\mathbf{R}_{\rm b})\,. \tag{19}$$

This is referred to as the hidden-scale-invariance condition. It can be shown that Eq. (18) is mathematically equivalent to Eq. (19) [84]. Equation (19) applies rigorously only for an Euler-homogeneous potential-energy function (Eq. (12)) plus a constant. Hidden scale invariance is easily checked in a simulation. Figure 11 shows in (a) data for the potential energies of scaled Lennard-Jones-Gaussian model configurations for which Eq. (19) is not a good approximation, and for comparison in (b) data for the exponentially repulsive pair potential where Eq. (19) works much better.

Because of continuity, Eq. (19) always applies to a good approximation for small density changes, so how does one judge to which degree hidden scale invariance applies. A quantitative measure for this is provided by the constant-density virial potential-energy Pearson correlation coefficient R defined [139, 140] as follows

$$R \equiv \frac{\langle \Delta U \Delta W \rangle}{\sqrt{\langle (\Delta U)^2 \rangle \langle (\Delta W)^2 \rangle}}\,. \tag{20}$$

Here W is the microscopic virial defined in Eq. (4), the thermal average of which (also denoted by W) obeys Eq. (3). In general, $-1 \le R \le 1$. If Eq. (18) applies rigorously, one has $R = 1$ (in exotic cases, $R = -1$ [141]). This is because at any given density knowledge of $U(\mathbf{R})$ via Eq. (18) implies knowledge of $S_{\rm ex}(\tilde{\mathbf{R}})$, which determines the virial via the analog of Eq. (18), $W(\mathbf{R}) = W(\rho, S_{\rm ex}(\tilde{\mathbf{R}}))$ (this expression follows from the definition $W(\mathbf{R}) \equiv (\partial U(\mathbf{R})/\partial \ln \rho)_{\tilde{\mathbf{R}}}$ [13]). Thus if R is close to unity, the hidden-scale-invariance condition Eq. (19) applies to a good approximation and Newton's equation of motion Eq. (14) is approximately invariant along the configurational adiabats. The criterion $R > 0.9$ has

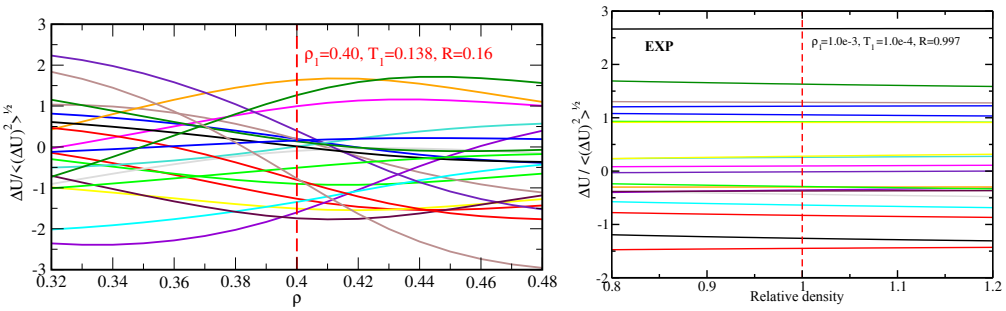

FIG. 11. Potential energies of configurations generated by uniform scaling of equilibrium configurations. At each density the average potential energy was subtracted, after which the data were normalized to unit variance. Equation (19) applies to a good approximation if the curves rarely cross one another. (a) Data for the Lennard-Jones Gaussian model with twenty configurations selected from an equilibrium simulation scaled uniformly ±20% in density [84]. There are several crossings, showing that Eq. (19) does not apply very well. Reproduced with permission from Ref. 84; copyright 2014 AIP Publishing. (b) Similar data for the exponentially repulsive pair potential system [138].

been used for defining the class of "strongly correlating systems" [139, 140, 142, 143], which to avoid confusion with strongly correlating quantum systems have been termed "Roskilde (R)-simple" systems [41, 144–157]. These are the systems that obey hidden scale invariance to a good approximation.

All systems have lines in the thermodynamic phase diagram of constant excess entropy. For R-simple systems these lines are termed isomorphs [14, 158] because the reduced-unit structure and dynamics are invariant to a good approximation along isomorphs.

VIII. BEYOND EXCESS-ENTROPY SCALING

We have argued that the simplest explanation of excess-entropy scaling is that the microscopic dynamics at state points with same excess entropy are virtually the same. If this applies, the system in question has hidden scale invariance (Eq. (19)). This property, however, only applies approximately and only for certain systems, and even for these it applies only in part of the thermodynamic phase diagram. This explains why excess-entropy scaling is neither exact nor universal. The class of R-simple systems – those obeying hidden scale invariance – is believed to include most metals and van der Waals bonded systems,

but exclude most systems with strong directional bonds like hydrogen-bonded or covalently bonded systems [158]. Ionic and dipolar systems constitute in-between cases that may or may not exhibit hidden scale invariance, depending on how strong the Coulomb forces are [158–161]. Whenever hidden scale invariance applies, however, it has a number of interesting consequences beyond those of the classical excess-entropy scaling of transport coefficients. The present section gives a few examples of this.

While Rosenfeld originally proposed excess-entropy scaling for single-component liquids of point-like particles interacting via pairwise additive forces, hidden scale invariance applies equally well to mixtures [100, 162, 163], non pair-force systems, confined system, molecular systems, and solids. For molecules, Eq. (19) relates to a uniform scaling of the center-of-mass coordinates, while orientations and molecular sizes are kept fixed. An example of isomorph-invariant dynamics was given in Fig. 4(c) reporting simulations of a liquid of ten-bead flexible Lennard-Jones chain molecules.

Isomorph invariance of the dynamics implies that a uniform scaling of a configuration selected from an equilibrated simulation at one state point results in an equilibrium configuration corresponding to a state point of different density and temperature (with the same excess entropy) [14]. Such a scaling is referred to as an "isomorph jump" because the system jumps instantaneously from equilibrium to equilibrium along an isomorph, in effect creating a wormhole in the thermodynamic phase diagram [14]. Two examples of this are provided in Fig. 12 showing in (a) an isomorph jump for a united-atom model of ortho-terphenyl and in (b) for a gold crystal. The latter illustrates that hidden scale invariance is not limited to the liquid phase; in fact, although this has not yet been studied very much, isomorph-theory predictions appear to apply equally well for solids as for liquids [166, 167].

A recent application of the isomorph theory was to quantify the thermodynamics of melting. For R-simple systems the melting line is an approximate isomorph [14, 150, 167, 168]. Via first-order Taylor expansions this fact makes it possible to predict from simulations carried out at a single coexistence state point the variation along the melting line of quantities like pressure, density, heat of melting, viscosity, Lindemann ratio, etc [167]. Examples are given for the LJ system in Fig. 13, in which the red curves are theoretical predictions based on simulations at $T = 2$ and the black dots are numerical data.

The isomorph theory has been applied to rationalize results from computer simulations of single-component and binary LJ-type systems [14, 169, 170], simple molecular models

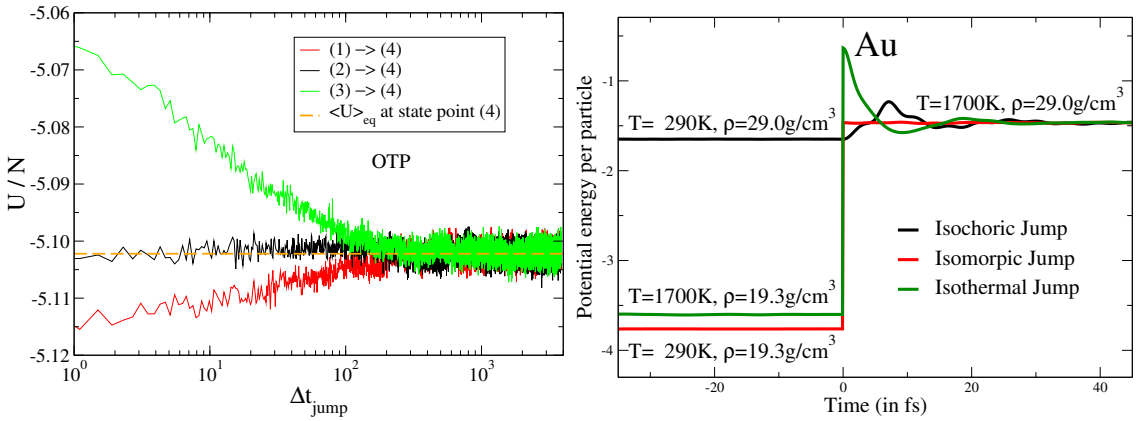

FIG. 12. Isomorph jumps monitored in NVT simulations. Isomorphs are traced out numerically in the phase diagram using Eq. (11) in a step-by-step fashion, typically involving a density variation of 1%. (a) Relaxation of the potential energy towards its equilibrium value after three jumps at $t = 0$ in the thermodynamic phase diagram for the viscous Lewis-Wahnström ortho-terphenyl model [164]. The black curve is for a jump between two state points on the same isomorph; here there is, after an initial instantaneous jump in potential energy (not visible), no subsequent slow relaxation towards equilibrium. The red and green curves are for non-isomorph jumps. Reproduced with permission from Ref. 25. (b) Same after jumps from three different state points of a face-centered cubic crystal of gold modeled via a realistic effective medium non-pair potential. Only the jump from a state point located on the final state point's isomorph (red curve) leads to instantaneous equilibration. Reproduced with permission from Ref. 165.

[25], crystals [166], nano-confined liquids (compare Fig. 5(b)) [33], non-linear shear flows [171], zero-temperature plastic flows of glasses [172], polymer-like flexible molecules (compare Fig. 4(c)) [30, 173], metals studied by *ab initio* density-functional-theory computer simulations [174], plasmas [175], physical aging [176], and justifying a quasiuniversal viscosity equation for supercritical R-simple liquids [65].

Experimental confirmations of isomorph-theory predictions were presented for van der Waals bonded liquids in Refs. 59, 177–179. As an example, the isomorph theory predicts with no free parameters how much the dielectric loss is suppressed by application of pressure (Fig. 14). For hydrogen-bonded liquids the theory does not work [59, 180], though; this confirms findings from simulations of water and methanol [140].

On the theoretical side, the isomorph theory led to "NVU molecular dynamics" defined

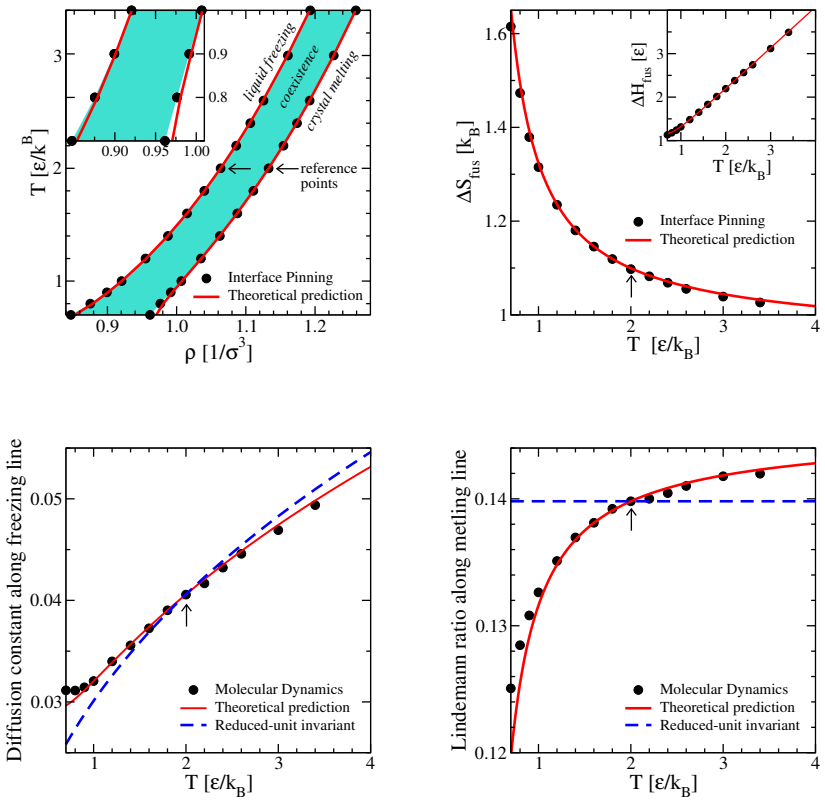

FIG. 13. The hidden scale invariance of the Lennard-Jones system leads to quantitative predictions for the variation along the melting line of the system's density, melting entropy, diffusion constant, and Lindemann ratio. Red lines are isomorph-theory predictions with all free parameters determined from simulations carried out at $T = 2$ (marked by arrows); black dots are simulation results. (a) The freezing and melting lines in the density-temperature phase diagram; the colored area marks the coexistence region. The triple point of the Lennard-Jones system is at $T \cong 0.7$. Close to it there are small deviations from the theoretical prediction, which are also apparent in (d). Reproduced with permission from Ref. 167. (b) The melting entropy along the freezing line, which is a constant in the simplest melting theories. Reproduced with permission from Ref. 167. (c) The liquid-state diffusion constant. The blue dashed line is the prediction if the reduced diffusion constant were constant, i.e., if the melting line were an exact isomorph. Reproduced with permission from Ref. 167. (d) The crystal's vibrational mean-square displacement relative to the interatomic spacing, the so-called Lindemann ratio. Reproduced with permission from Ref. 167.

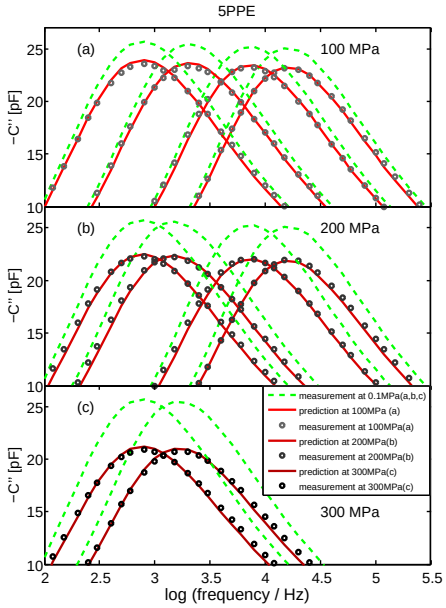

FIG. 14. The frequency-dependent dielectric losses $C''(f)$ measured at different temperatures at ambient pressure (green dashed lines), from which the losses at corresponding isochronal states are predicted. Data are shown for (a) 100MPa, (b) 200MPa, (c) 300MPa [178]. The red curves are the isomorph-theory predicted high-pressure dielectric losses (no free parameters), the black dots are high-pressure data. Reproduced with permission from Ref. 178; copyright 2015 Elsevier.

as motion at a constant velocity along geodesic curves on the high-dimensional constant-potential-energy hypersurface [181–183]. Despite the fact that the potential and kinetic energies are both strictly conserved in NVU dynamics, this novel dynamics gives results that are for most quantities identical to those obtained by standard NVE or NVT Newtonian dynamics [182]. The isomorph theory has also been applied to formulate a theoretical tool, the "isomorph filter", according to which any universally valid theory for the relaxation time of glass-forming liquids must be based on isomorph-invariant quantities since the (reduced) relaxation time is itself an isomorph invariant. This makes it possible to rule out a number of well-known models [14].

According to the standard explanation of quasiuniversality, two systems have the same structure and dynamics to a good approximation if they correspond to hard-sphere systems with the same packing fraction [1, 3, 4]. Rosenfeld realized that this translates into the two systems having the same excess entropy. The isomorph theory has recently made it possible to derive simple liquids' quasiuniversality without reference to the hard-sphere system. The

proof is based on using the exponentially repulsive pair-potential system as a reference system [15, 184]. Different simple liquids with the same $S_{\rm ex}$ have virtually the same structure and dynamics because they have virtually the same reduced-coordinate potential-energy function, and this function is conveniently identified with that of the exponentially repulsive pair-potential system [185]. Systems that are quasiuniversal are those for which the pair potential may be approximated by a finite sum of exponentially repulsive pair potentials with prefactors that in reduced units are numerically much larger than unity [15, 184]. This provides a method for determining which pair-potential systems are quasiuniversal and which are not.

Maimbourgh and Kurchan recently showed that for systems with strong repulsive forces, the isomorph theory is exact in infinite dimensions [186]. This suggests the intriguing scenario that excess-entropy scaling is a finite-dimensional manifestation of a high-dimensional regularity and that, consequently, deviations from excess-entropy scaling should be quantified via a suitable expansion in $1/d$ in which d is the spatial dimension [170]. – Readers further interested in the isomorph theory are referred to the reviews Refs. 15, 143, 158, and 161.

IX. CONCLUDING REMARKS

Rosenfeld's discovery of excess-entropy scaling more than forty years ago was based on that time's primitive computer simulations. It provides an early example of a theoretical insight generated by simulation results that preceded experimental confirmation. Rosenfeld's explanation of excess-entropy scaling was based on the fact that simple liquids have virtually the same physics as the hard-sphere system. Thus he viewed excess-entropy scaling as a *confirmation* of quasiuniversality and, in particular, as a demonstration that quasiuniversality applies not just to structure, but also to dynamics [1, 187–189].

The hard-sphere system has a trivial potential-energy function, which is either zero or infinite, whereas the scaling properties of $U(\mathbf{R})$ are central in isomorph theory. Despite this fundamental difference, the isomorph theory is entirely compatible with Rosenfeld's explanation of excess-entropy scaling based on simple liquids' quasiuniversality. But while Rosenfeld explained excess-entropy scaling from quasiuniversality, the isomorph theory in a sense does the opposite and explains quasiuniversality from the exponentially repulsive

pair-potential system's hidden scale invariance [15, 184].

For the hard-sphere system, the packing fraction determines quantities like the reduced diffusion constant, viscosity, and thermal conductivity [1]. While many suggestions exist for how to determine the equivalent HS-system packing fraction of a simple liquid at a given state point [190–198], Rosenfeld's idea was to refer instead to the system's excess entropy, a purely thermodynamic quantity that for the hard-sphere system is in a one-to-one correspondence with the packing fraction [5, 199]. This is how excess-entropy scaling was arrived at; it also led to the proposition of a universal $S_{\rm ex}$ dependence of the reduced transport coefficients [1]. The exponential $S_{\rm ex}$ dependence of Rosenfeld scaling Eq. (8) was not justified theoretically in Ref. 1, but reported as an approximate empirical fact, and it is now known to apply only in some instances of excess-entropy scaling.

The basic message of hidden scale invariance is the irrelevance of the pair potential's characteristic length scale [158]. The Lennard-Jones potential-energy minimum is found at the pair distance $r = 2^{1/6}\sigma$ in which σ is the characteristic lenght of the LJ pair potential. If the average nearest-neighbor distance is close to this value, the pressure is small. Hidden scale invariance reflects the non-trivial fact that the length σ is irrelevant for the physics [15, 161] because the pressure is irrelevant for the reduced-unit structure and dynamics. In contrast, for the hard-sphere system the virial part of the pressure is determined by the packing fraction (equivalently: the excess entropy), and the pressure determines the excess entropy and the dynamical properties [199].

A quantitative measure of how well hidden scale invariance applies for a given system is provided by the virial potential-energy correlation coefficient R of Eq. (20). Whenever R is close to unity, excess-entropy scaling applies to a good approximation. If this is the case, the system obeys isochronal superposition, the property that two different state points of a given system with, e.g., the same dielectric loss-peak frequency have the same reduced relaxation functions [26, 27, 180].

Isomorph theory is not limited to explaining excess-entropy scaling for single-component pair-potential liquids, it applies also for solids, non-pair potential systems, mixtures, molecules, confined systems, aging systems, etc. Note that S_2, as well as the higher-order configurational entropies (Eq. (9)), are all isomorph invariant because the reduced-unit structure is. This means that for tracing out the lines of invariant dynamics, i.e., the isomorphs, instead of keeping $S_{\rm ex}$ constant one might equally well keep S_2, S_3, or the so-called

residual multiparticle excess entropy $S_{\rm RMPE} \equiv S_{\rm ex} - S_2$ constant [53, 200].

Isomorph theory explains why excess-entropy scaling applies also for molecular systems quite different from the quasiuniversal simple point-particle liquids traditionally studied in liquid-state theory [5]. The above "derivation" of isomorph theory from excess-entropy scaling showed that if the phase diagram has lines of invariant structure and dynamics, these lines must be the configurational adiabats, i.e., that excess-entropy scaling must apply.

It must be emphasized that far from all observations of this field of research are explained by the isomorph theory. Rosenfeld scaling Eq. (8) cannot be derived from the hidden-scale-invariance condition Eq. (19), which is not surprising given that there are several cases of excess-entropy scaling for which Rosenfeld scaling does not apply. Moreover, excess-entropy scaling or closely related regularities have been observed to apply also for a number of systems that do not have strong virial potential-energy correlations [35, 51, 103, 133, 134]. Isomorph theory cannot explain this, at least not in its present version. There are examples of systems, e.g., with vibrational degrees of freedom modeled by harmonic springs, which do not have strong virial potential-energy correlations, but which can be coarse-grained into a system that obeys isomorph theory by replacing harmonic molecular bonds by rigid bonds [173]. More work is needed to clarify to which extent coarse-graining may lead to hidden scale invariance of the remaining degrees of freedom. It remains an open question whether hidden scale invariance in one form or the other will eventually be able to provide a full explanation of excess-entropy scaling and related regularities.

ACKNOWLEDGMENTS

The author is indebted to Nick Bailey, Lorenzo Costigliola, Jack Douglas, Trond Ingebrigtsen, and Kristine Niss for suggestions improving the presentation. Heine Larsen provided invaluable technical assistance. This work was supported by the VILLUM Foundation's *Matter* grant (No. 16515).

[1] Y. Rosenfeld, "Relation between the Transport Coefficients and the Internal Entropy of Simple Systems," Phys. Rev. A **15**, 2545–2549 (1977).

[2] J. E. Lennard-Jones, "On the Determination of Molecular Fields. I. From the Variation of the Viscosity of a Gas with Temperature," Proc. R. Soc. London A **106**, 441–462 (1924).

[3] B. Widom, "Intermolecular forces and the nature of the liquid state," Science **157**, 375–382 (1967).

[4] D. Chandler, J. D. Weeks, and H. C. Andersen, "Van der Waals picture of liquids, solids, and phase transformations," Science **220**, 787–794 (1983).

[5] J.-P. Hansen and I. R. McDonald, *Theory of Simple Liquids: With Applications to Soft Matter*, 4th ed. (Academic, New York, 2013).

[6] J. D. Weeks, D. Chandler, and H. C. Andersen, "Role of repulsive forces in determining the equilibrium structure of simple liquids," J. Chem. Phys. **54**, 5237–5247 (1971).

[7] J. A. Barker and D. Henderson, "What is "liquid"? Understanding the states of matter," Rev. Mod. Phys. **48**, 587–671 (1976).

[8] W. G. Hoover, *Molecular Dynamics*, Lecture Notes in Physics No. 258 (Springer, 1986).

[9] Y. Rosenfeld, "A quasi-universal scaling law for atomic transport in simple fluids," J. Phys.: Condens. Matter **11**, 5415–5427 (1999).

[10] L. E. Reichl, *A Modern Course in Statistical Physics*, 4th ed. (Wiley-VCH, 2016).

[11] T. B. Schrøder and J. C. Dyre, "ac hopping conduction at extreme disorder takes place on the percolating cluster," Phys. Rev. Lett. **101**, 025901 (2008).

[12] L. D. Landau and E. M. Lifshitz, *Statistical Physics* (Pergamon, Oxford, 1958).

[13] M. P. Allen and D. J. Tildesley, *Computer Simulation of Liquids* (Oxford Science Publications, 1987).

[14] N. Gnan, T. B. Schrøder, U. R. Pedersen, N. P. Bailey, and J. C. Dyre, "Pressure-Energy Correlations in Liquids. IV. "Isomorphs" in Liquid Phase Diagrams," J. Chem. Phys. **131**, 234504 (2009).

[15] J. C. Dyre, "Simple liquids' quasiuniversality and the hard-sphere paradigm," J. Phys. Condens. Matter **28**, 323001 (2016).

[16] K. R. Harris, "Scaling the transport properties of molecular and ionic liquids," J. Molec. Liq. **222**, 520–534 (2016).

[17] E. N. C. Andrade, "XLI. A theory of the viscosity of liquids. – Part I," The London, Edinburgh, and Dublin Philosophical Magazine and Journal of Science **17**, 497–511 (1934).

[18] W. Kob and H. C. Andersen, "Testing mode-coupling theory for a supercooled binary

Lennard-Jones mixture I: The van Hove correlation function," Phys. Rev. E **51**, 4626–4641 (1995).

[19] M. Agarwal, M. Singh, B. S. Jabes, and C. Chakravarty, "Excess entropy scaling of transport properties in network-forming ionic melts (SiO_2 and BeF_2)," J. Chem. Phys. **134**, 014502 (2011).

[20] Q.-L. Cao, D.-H. Huang, J.-S. Yang, M.-J. Wan, and F.-H. Wang, "Transport properties and the entropy-scaling law for liquid tantalum and molybdenum under high pressure," Chinese Phys. Lett. **31**, 066202 (2014).

[21] U. R. Pedersen, T. B. Schrøder, and J. C. Dyre, "Phase diagram of Kob-Andersen-type binary Lennard-Jones mixtures," Phys. Rev. Lett. **120**, 165501 (2018).

[22] S. Korkmaz, U. U. N. Yazar, and S. D. Korkmaz, "A comparative study of the atomic transport properties of liquid alkaline metals using scaling laws," Fluid Phase Equilibria **249**, 159 – 164 (2006).

[23] R. Chopra, T. M. Truskett, and J. R. Errington, "On the use of excess entropy scaling to describe single-molecule and collective dynamic properties of hydrocarbon isomer fluids," J. Phys. Chem. B **114**, 16487–16493 (2010).

[24] R. Chopra, T. M. Truskett, and J. R. Errington, "Excess entropy scaling of dynamic quantities for fluids of dumbbell-shaped particles," J. Chem. Phys. **133**, 104506 (2010).

[25] T. S. Ingebrigtsen, T. B. Schrøder, and J. C. Dyre, "Isomorphs in model molecular liquids," J. Phys. Chem. B **116**, 1018–1034 (2012).

[26] C. M. Roland, R. Casalini, and M. Paluch, "Isochronal temperature–pressure superpositioning of the alpha–relaxation in type-A glass formers," Chem. Phys. Lett. **367**, 259–264 (2003).

[27] K. L. Ngai, R. Casalini, S. Capaccioli, M. Paluch, and C. M. Roland, "Do theories of the glass transition, in which the structural relaxation time does not define the dispersion of the structural relaxation, need revision?" J. Phys. Chem. B **109**, 17356–17360 (2005).

[28] G. Galliero, C. Boned, and J. Fernandez, "Scaling of the viscosity of the Lennard-Jones chain fluid model, argon, and some normal alkanes," J. Chem. Phys. **134**, 064505 (2011).

[29] G. Galliero and C. Boned, "Thermal conductivity of the Lennard-Jones chain fluid model," Phys. Rev. E **80**, 061202 (2009).

[30] A. A. Veldhorst, J. C. Dyre, and T. B. Schrøder, "Scaling of the dynamics of flexible

Lennard-Jones chains," J. Chem. Phys. **141**, 054904 (2014).

[31] E. Voyiatzis, F. Muller-Plathe, and M. C Bohm, "Do transport properties of entangled linear polymers scale with excess entropy?" Macromolecules **46**, 8710–8723 (2013).

[32] J. Mittal, J. R. Errington, and T. M. Truskett, "Thermodynamics predicts how confinement modifies the dynamics of the equilibrium hard-sphere fluid," Phys. Rev. Lett. **96**, 177804 (2006).

[33] T. S. Ingebrigtsen, J. R Errington, T. M. Truskett, and J. C. Dyre, "Predicting how nanoconfinement changes the relaxation time of a supercooled liquid," Phys. Rev. Lett. **111**, 235901 (2013).

[34] Y. D. Fomin, V. N. Ryzhov, and N. V. Gribova, "Breakdown of excess entropy scaling for systems with thermodynamic anomalies," Phys. Rev. E **81**, 061201 (2010).

[35] R. Chopra, T. M. Truskett, and J. R. Errington, "On the use of excess entropy scaling to describe the dynamic properties of water," J. Phys. Chem. B **114**, 10558 (2010).

[36] V. V. Vasisht, J. Mathew, S. Sengupta, and S. Sastry, "Nesting of thermodynamic, structural, and dynamic anomalies in liquid silicon," J. Chem. Phys. **141**, 124501 (2014).

[37] S. Higuchi, D. Kato, D. Awaji, and K. Kim, "Connecting thermodynamic and dynamical anomalies of water-like liquid-liquid phase transition in the Fermi-Jagla model," J. Chem. Phys. **148**, 094507 (2018).

[38] Y. D. Fomin, E. N. Tsiok, and V. N. Ryzhov, "Core-softened system with attraction: Trajectory dependence of anomalous behavior," J. Chem. Phys. **135**, 124512 (2011).

[39] H.-O. May and P. Mausbach, "Thermodynamic excess properties and their scaling behavior for the Gaussian core model fluid," Fluid Phase Equilibria **313**, 156–164 (2012).

[40] R. Sharma, S. N. Chakraborty, and C. Chakravarty, "Entropy, diffusivity, and structural order in liquids with waterlike anomalies," J. Chem. Phys. **125**, 204501 (2006).

[41] S. Prasad and C. Chakravarty, "Onset of simple liquid behaviour in modified water models," J. Chem. Phys. **140**, 164501 (2014).

[42] D. Dhabal, C. Chakravarty, V. Molinero, and H. K. Kashyap, "Comparison of liquid-state anomalies in Stillinger-Weber models of water, silicon, and germanium," J. Chem. Phys. **145**, 214502 (2016).

[43] Q.-L. Cao, X.-S. Kong, Y. D. Li, X. Wu, and C. S. Liu, "Revisiting scaling laws for the diffusion coefficients in simple melts based on the structural deviation from hard-sphere-like

case," Physica B **406**, 3114–3119 (2011).

[44] V. Molinero and E. B. Moore, "Water modeled as an intermediate element between carbon and silicon," J. Phys. Chem. B **113**, 4008–4016 (2009).

[45] D. Dhabal, A. H. Nguyen, M. Singh, P. Khatua, V. Molinero, S. Bandyopadhyay, and C. Chakravarty, "Excess entropy and crystallization in Stillinger-Weber and Lennard-Jones fluids," J. Chem. Phys. **143**, 164512 (2015).

[46] H. S. Green, *The Molecular Theory of Fluids* (North- Holland, Amsterdam, 1952).

[47] A. Baranyai and D. J. Evans, "Direct entropy calculation from computer simulation of liquids," Phys. Rev. A **40**, 3817–3822 (1989).

[48] M. Dzugutov, "A universal scaling law for atomic diffusion in condensed matter," Nature **381**, 137–139 (1996).

[49] I. Yokoyama, "A relationship between excess entropy and diffusion coefficient for liquid metals near the melting point," Physica B **254**, 172–177 (1998).

[50] J. J. Hoyt, M. Asta, and B. Sadigh, "Test of the universal scaling law for the diffusion coefficient in liquid metals," Phys. Rev. Lett. **85**, 594–597 (2000).

[51] J. R. Errington, T. M. Truskett, and J. Mittal, "Excess-entropy-based anomalies for a waterlike fluid," J. Chem. Phys. **125**, 244502 (2006).

[52] Y. D. Fomin, V. N. Ryzhov, B. A. Klumov, and E. N. Tsiok, "How to quantify structural anomalies in fluids?" J. Chem. Phys. **141**, 034508 (2014).

[53] M. K. Nandi, A. Banerjee, S. Sengupta, S. Sastry, and S. M. Bhattacharyya, "Unraveling the success and failure of mode coupling theory from consideration of entropy," J. Chem. Phys. **143**, 174504 (2015).

[54] E. H. Abramson, "Viscosity of argon to 5 GPa and 673 K," High Pressure Research **31**, 544–548 (2011).

[55] E. H. Abramson, "Viscosity of carbon dioxide measured to a pressure of 8 GPa and temperature of 673 K," Phys. Rev. E **80**, 021201 (2009).

[56] E. H. Abramson, "Viscosity of methane to 6 GPa and 673 K," Phys. Rev. E **84**, 062201 (2011).

[57] R. V. Vaz, A. L. Magalhaes, D. L. A. Fernandes, and C. M. Silva, "Universal correlation of self-diffusion coefficients of model and real fluids based on residual entropy scaling law," Chem. Engn. Sci. **79**, 153–162 (2012).

[58] X. Ma, W. Chen, Z. Wang, Y. Peng, Y. Han, and P. Tong, "Test of the universal scaling law of diffusion in colloidal monolayers," Phys. Rev. Lett. **110**, 078302 (2013).

[59] H. W. Hansen, A. Sanz, K. Adrjanowicz, B. Frick, and K. Niss, "Evidence of a one-dimensional thermodynamic phase diagram for simple glass-formers," Nat. Commun. **9**, 518 (2018).

[60] Ian H. Bell, Jorrit Wronski, Sylvain Quoilin, and Vincent Lemort, "Pure and pseudo-pure fluid thermophysical property evaluation and the open-source thermophysical property library coolprop," Industrial & Engineering Chemistry Research **53**, 2498–2508 (2014), https://doi.org/10.1021/ie4033999.

[61] I. H. Bell, "Probing the link between residual entropy and viscosity of molecular fluids and model potentials," arXiv:1809.05682 (2018).

[62] K. Nygard, "Colloidal diffusion in confined geometries," Phys. Chem. Chem. Phys. **19**, 23632–23641 (2017).

[63] Y. Tian, X. Xu, and J. Wu, "Thermodynamic route to efficient prediction of gas diffusivity in nanoporous materials," Langmuir **33**, 11797–11803 (2017).

[64] H. O. Baled, I. K. Gamwo, R. M. Enick, and M. A. McHugh, "Viscosity models for pure hydrocarbons at extreme conditions: A review and comparative study," Fuel **218**, 89–111 (2018).

[65] L. Costigliola, U. R. Pedersen, D.M. Heyes, T. B. Schrøder, and J. C. Dyre, "Communication: Simple liquids' high-density viscosity," J. Chem. Phys. **148**, 081101 (2018).

[66] M. Hopp, J. Mele, and J. Gross, "Self-diffusion coefficients from entropy scaling using the PCP-SAFT equation of state," Ind. Eng. Chem. Res. **57**, 12942–12950 (2018).

[67] O. Lötgering-Lin, M. Fischer, M. Hopp, and J. Gross, "Pure substance and mixture viscosities based on entropy scaling and an analytic equation of state," Ind. Eng. Chem. Res. **57**, 4095–4114 (2018).

[68] S. Bastea, "Thermodynamics and diffusion in size-symmetric and asymmetric dense electrolytes," J. Chem. Phys. **135**, 084515 (2011).

[69] G. Goel, D. J. Lacks, and J. A. Van Orman, "Transport coefficients in silicate melts from structural data via a structure-thermodynamics-dynamics relationship," Phys. Rev. E **84**, 051506 (2011).

[70] F. Jia, T. Yun, and W. Jianzhong, "Classical density functional theory for methane adsorp-

tion in metal-organic framework materials," AIChE Journal **61**, 3012–3021 (2015).

[71] Y. Liu, F. Guo, J. Hu, S. Zhao, H. Liu, and Y. Hu, "Entropy prediction for H_2 adsorption in metal-organic frameworks," Phys. Chem. Chem. Phys. **18**, 23998–24005 (2016).

[72] W. A. Fouad and L. F. Vega, "Transport properties of HFC and HFO based refrigerants using an excess entropy scaling approach," J. Supercrit. Fluids **131**, 106 – 116 (2018).

[73] M. Hopp and J. Gross, "Thermal conductivity of real substances from excess entropy scaling using PCP-SAFT," Ind. Eng. Chem. Res. **56**, 4527–4538 (2017).

[74] Q.-L. Cao, P.-P. Wang, J.-X. Shao, and F.-H. Wang, "Transport properties and entropy-scaling laws for diffusion coefficients in liquid $Fe_{0.9}Ni_{0.1}$ up to 350 GPa," RSC Adv. **6**, 84420–84425 (2016).

[75] Y. Liu, J. Fu, and J. Wu, "Excess-entropy scaling for gas diffusivity in nanoporous materials," Langmuir **29**, 12997–13002 (2013).

[76] Y. Tian, W. Fei, and J. Wu, "Separation of carbon isotopes in methane with nanoporous materials," Ind. Eng. Chem. Res. **57**, 5151–5160 (2018).

[77] L. T. Novak, "Predictive corresponding-states viscosity model for the entire fluid region: n-alkanes," Ind. Eng. Chem. Res. **52**, 6841–6847 (2013).

[78] J. N. Dahanayake and K. R. Mitchell-Koch, "Entropy connects water structure and dynamics in protein hydration layer," Phys. Chem. Chem.Phys. **20**, 14765–14777 (2018).

[79] P. He, H. Li, and X. Hou, "Excess-entropy scaling of dynamics for methane in various nanoporous materials," Chem. Phys. Lett. **593**, 83–88 (2014).

[80] O. Lötgering-Lin and J. Gross, "Group contribution method for viscosities based on entropy scaling using the perturbed-chain polar statistical associating fluid theory," Ind. Eng. Chem. Res. **54**, 7942–7952 (2015).

[81] J. Gross and G. Sadowski, "Perturbed-chain SAFT: An equation of state based on a perturbation theory for chain molecules," Ind. Eng. Chem. Res. **40**, 1244–1260 (2001).

[82] Y. Hiwatari, H. Matsuda, T. Ogawa, N. Ogita, and A. Ueda, "Molecular dynamics studies on the soft-core model," Prog. Theor. Phys. **52**, 1105–1123 (1974).

[83] S. Pieprzyk, D. M. Heyes, and A. C. Branka, "Thermodynamic properties and entropy scaling law for diffusivity in soft spheres," Phys. Rev. E **90**, 012106 (2014).

[84] T. B. Schrøder and J. C. Dyre, "Simplicity of condensed matter at its core: Generic definition of a Roskilde-simple system," J. Chem. Phys. **141**, 204502 (2014).

[85] W. G. Hoover, S. G. Gray, and K. W. Johnson, "Thermodynamic properties of the fluid and solid phases for inverse power potentials," J. Chem. Phys. **55**, 1128–1136 (1971).

[86] A. C. Branka and D. M. Heyes, "Thermodynamic properties of inverse power fluids," Phys. Rev. E **74**, 031202 (2006).

[87] A. C. Branka and D. M. Heyes, "Pair correlation function of soft-sphere fluids," J. Chem. Phys. **134**, 064115 (2011).

[88] J. Mittal, J. R. Errington, and T. M. Truskett, "Relationships between self-diffusivity, packing fraction, and excess entropy in simple bulk and confined fluids," J. Phys. Chem. B **111**, 10054–10063 (2007).

[89] B. Lautrup, *Physics of Continuous Matter*, 2nd ed. (CRC Press, 2011).

[90] N. Jakse and A. Pasturel, "Excess entropy scaling law for diffusivity in liquid metals," Scientific Reports **6**, 20689 (2016).

[91] S. Chapman and T. G. Cowling, *The mathematical theory of non-uniform gases: An account of the kinetic theory of viscosity, thermal conduction and diffusion in gases* (Cambridge University Press, 1970).

[92] N. S. Krylov, *Works on the Foundations of Statistical Physics* (Princeton University Press, 1979).

[93] P. Billingsley, *Ergodic Theory and Information* (Wiley, 1965).

[94] P. Allegrini, J. F. Douglas, and S. C. Glotzer, "Dynamic entropy as a measure of caging and persistent particle motion in supercooled liquids," Phys. Rev. E **60**, 5714–5724 (1999).

[95] M. Dzugutov, E. Aurell, and A. Vulpiani, "Universal relation between the Kolmogorov-Sinai entropy and the thermodynamical entropy in simple liquids," Phys. Rev. Lett. **81**, 1762–1765 (1998).

[96] H. Pang, Y. Shin, D. Ihm, E. K. Lee, and O. Kum, "Correlation between the Kolmogorov-Sinai entropy and the self-diffusion coefficient in simple liquids," Phys. Rev. E **62**, 6516–6521 (2000).

[97] A. Samanta, S. M. Ali, and S. K. Ghosh, "New universal scaling laws of diffusion and Kolmogorov-Sinai entropy in simple liquids," Phys. Rev. Lett. **92**, 145901 (2004).

[98] S. Bastea, "Entropy scaling laws for diffusion," Phys. Rev. Lett. **93**, 199603 (2004).

[99] W. Götze, *Complex dynamics of glass-forming liquids: A mode-coupling theory* (Oxford University Press, 2008).

[100] A. Samanta, S. M. Ali, and S. K. Ghosh, "Universal scaling laws of diffusion in a binary fluid mixture," Phys. Rev. Lett. , 245901 (2001).

[101] P. Gallo and M. Rovere, "Relation between the two-body entropy and the relaxation time in supercooled water," Phys. Rev. E **91**, 012107 (2015).

[102] W. P Krekelberg, M. J. Pond, G. Goel, V. K. Shen, J. R. Errington, and T. M. Truskett, "Generalized Rosenfeld scalings for tracer diffusivities in not-so-simple fluids: Mixtures and soft particles," Phys. Rev. E **80**, 061205 (2009).

[103] W. P. Krekelberg, T. Kumar, J. Mittal, J. R. Errington, and T. M. Truskett, "Anomalous structure and dynamics of the Gaussian-core fluid," Phys. Rev. E **79**, 031203 (2009).

[104] M. J. Pond, J. R. Errington, and T. M. Truskett, "Generalizing Rosenfeld's excess-entropy scaling to predict long-time diffusivity in dense fluids of Brownian particles: From hard to ultrasoft interactions," J. Chem. Phys. **134**, 081101 (2011).

[105] M. Goldstein, "Viscous liquids and the glass transition: A potential energy barrier picture," J. Chem. Phys. **51**, 3728–3739 (1969).

[106] P. G. Wolynes, "Randomness and complexity in chemical physics," Acc. Chem. Res. **25**, 513–519 (1992).

[107] F. H. Stillinger and T. A. Weber, "Dynamics of structural transitions in liquids," Phys. Rev. A **28**, 2408–2416 (1983).

[108] T. A. Weber and F. H. Stillinger, "Local order and structural transitions in amorphous metal-metalloid alloys," Phys. Rev. B **31**, 1954–1963 (1985).

[109] S. Sastry, P. G. Debenedetti, and F. H. Stillinger, "Signatures of distinct dynamical regimes in the energy landscape of a glass-forming liquid," Nature **393**, 554–557 (1998).

[110] B. Derrida, "Random-energy model: Limit of a family of disordered models," Phys. Rev. Lett. **45**, 79–82 (1980).

[111] R. Zwanzig, "Diffusion in a rough potential," PNAS **85**, 2029–2030 (1988).

[112] J. C. Dyre, "Energy master equation: A low-temperature approximation to Bässler's random-walk model," Phys. Rev. B **51**, 12276–12294 (1995).

[113] S. S. Plotkin, J. Wang, and P. G. Wolynes, "Correlated energy landscape model for finite, random heteropolymers," Phys. Rev. E **53**, 6271–6296 (1996).

[114] S. Banerjee, R. Biswas, K. Seki, and B. Bagchi, "Diffusion on a rugged energy landscape with spatial correlations," J. Chem. Phys. **141**, 124105 (2014).

[115] K. Seki and B. Bagchi, "Relationship between entropy and diffusion: A statistical mechanical derivation of Rosenfeld expression for a rugged energy landscape," J. Chem. Phys. **143**, 194110 (2015).

[116] J. H. Gibbs and E. A. DiMarzio, "Nature of the glass transition and the glassy state," J. Chem. Phys. **28**, 373–383 (1958).

[117] A. B. Bestul and S. S. Chang, "Excess entropy at glass transformation," J. Chem. Phys. **40**, 3731–3733 (1964).

[118] G. Adam and J. H. Gibbs, "On temperature dependence of cooperative relaxation properties in glass-forming liquids," J. Chem. Phys. **43**, 139–146 (1965).

[119] F. Simon, "Über den Zustand der unterkühlten Flüssigkeiten und Glässer," Z. Anorg. Allg. Chem. **203**, 219–227 (1931).

[120] W. Kauzmann, "The nature of the glassy state and the behavior of liquids at low temperatures," Chem. Rev. **43**, 219 (1948).

[121] L.-M. Martinez and C. A. Angell, "A thermodynamic connection to the fragility of glass-forming liquids," Nature **410**, 663–667 (2001).

[122] J. Dudowicz, K. F. Freed, and J. F. Douglas, "Generalized entropy theory of polymer glass formation," Adv. Chem. Phys. **137**, 125–222 (2008).

[123] W.-S. Xu and K. F. Freed, "Thermodynamic scaling of dynamics in polymer melts: Predictions from the generalized entropy theory," J. Chem. Phys. **138**, 234501 (2013).

[124] S. N. Chakraborty and C. Chakravarty, "Diffusivity, excess entropy, and the potential-energy landscape of monatomic liquids," J. Chem. Phys. **124**, 014507 (2006).

[125] M. S. Shell, "Coarse-graining with the relative entropy," in *Adv. Chem. Phys.*, Vol. 161, edited by S. A. Rice and A. R. Dinner (John Wiley & Sons, Inc., 2016) pp. 395–441.

[126] S. Kullback and R. A. Leibler, "On information and sufficiency," Ann. Math. Stat. **22**, 79–86 (1951).

[127] M. S. Shell, "Systematic coarse-graining of potential energy landscapes and dynamics in liquids," J. Chem. Phys. **137**, 084503 (2012).

[128] P. K. Kovtun, D. T. Son, and A. O. Starinets, "Viscosity in strongly interacting quantum field theories from black hole physics," Phys. Rev. Lett. **94**, 111601 (2005).

[129] J. Zaanen, "Planckian dissipation, minimal viscosity and the transport in cuprate strange metals," arXiv:1807.10951 (2018).

[130] G. G. N. Angilella, N. H. March, F. M. D. Pellegrino, and R. Pucci, "Proposed lower bound for the shear viscosity to entropy density ratio in some dense liquids," Phys. Lett. A **373**, 992–998 (2009).

[131] G. Faussurier, S. B. Libby, and P. L. Silvestrelli, "The viscosity to entropy ratio: From string theory motivated bounds to warm dense matter transport," High Energy Density Physics **12**, 21–26 (2014).

[132] U. Hohm, "On the ratio of the shear viscosity to the density of entropy of the rare gases and H_2, N_2, CH_4, and CF_4," Chem. Phys. **444**, 39–42 (2014).

[133] M. Agarwal, M. Singh, R. Sharma, M. P. Alam, and C. Chakravarty, "Relationship between structure, entropy, and diffusivity in water and water-like liquids," J. Phys. Chem. B **114**, 6995–7001 (2010).

[134] D. Nayar and C. Chakravarty, "Water and water-like liquids: Relationships between structure, entropy and mobility," Phys. Chem. Chem. Phys. **15**, 14162–14177 (2013).

[135] W. P. Krekelberg, V. Ganesan, and T. M. Truskett, "Shear-rate-dependent structural order and viscosity of a fluid with short-range attractions," Phys. Rev. E **78**, 010201 (2008).

[136] W. P. Krekelberg, V. Ganesan, and T. M. Truskett, "Structural signatures of mobility on intermediate time scales in a supercooled fluid," J. Chem. Phys. **132**, 184503 (2010).

[137] T. S. Ingebrigtsen and H. Tanaka, "Structural predictor for nonlinear sheared dynamics in simple glass-forming liquids," PNAS **115**, 87–92 (2018).

[138] A. K. Bacher, T. B. Schrøder, and J. C. Dyre, "The EXP pair-potential system. II. Fluid phase isomorphs," J. Chem. Phys. **149**, 114502 (2018).

[139] U. R. Pedersen, N. P. Bailey, T. B. Schrøder, and J. C. Dyre, "Strong Pressure-Energy Correlations in van der Waals Liquids," Phys. Rev. Lett. **100**, 015701 (2008).

[140] N. P. Bailey, U. R. Pedersen, N. Gnan, T. B. Schrøder, and J. C. Dyre, "Pressure-Energy Correlations in Liquids. I. Results from Computer Simulations," J. Chem. Phys. **129**, 184507 (2008).

[141] C. Ruscher, J. Baschnagel, and J. Farago, "The Voronoi liquid," EPL (Europhysics Letters) **112**, 66003 (2015).

[142] N. P. Bailey, U. R. Pedersen, N. Gnan, T. B. Schrøder, and J. C. Dyre, "Pressure-Energy Correlations in Liquids. II. Analysis and Consequences," J. Chem. Phys. **129**, 184508 (2008).

[143] U. R. Pedersen, N. Gnan, N. P. Bailey, T. B. Schrøder, and J. C. Dyre, "Strongly correlating

liquids and their isomorphs," J. Non-Cryst. Solids **357**, 320–328 (2011).

[144] A. Malins, J. Eggers, and C. P. Royall, "Investigating isomorphs with the topological cluster classification," J. Chem. Phys. **139**, 234505 (2013).

[145] E. H. Abramson, "Viscosity of fluid nitrogen to pressures of 10 GPa," J. Phys. Chem. B **118**, 11792–11796 (2014).

[146] J. Fernandez and E. R. Lopez, "Experimental thermodynamics: Advances in transport properties of fluids," (Royal Society of Chemistry, 2014) Chap. 9.3, pp. 307–317.

[147] E. Flenner, H. Staley, and G. Szamel, "Universal Features of Dynamic Heterogeneity in Supercooled Liquids," Phys. Rev. Lett. **112**, 097801 (2014).

[148] U. Buchenau, "Thermodynamics and dynamics of the inherent states at the glass transition," J. Non-Cryst. Solids **407**, 179–183 (2015).

[149] K. R. Harris and M. Kanakubo, "Self-diffusion, velocity cross-correlation, distinct diffusion and resistance coefficients of the ionic liquid [BMIM][Tf2N] at high pressure," Phys. Chem. Chem. Phys. **17**, 23977–23993 (2015).

[150] D. M. Heyes, D. Dini, and A. C. Branka, "Scaling of Lennard-Jones liquid elastic moduli, viscoelasticity and other properties along fluid-solid coexistence," Phys. Status Solidi (b) **252**, 1514–1525 (2015).

[151] J. W. P. Schmelzer and T. V. Tropin, "Kinetic criteria of glass-formation, pressure dependence of the glass-transition temperature, and the Prigogine–Defay ratio," J. Non-Cryst. Solids **407**, 170–178 (2015).

[152] K. Adrjanowicz, M. Paluch, and J. Pionteck, "Isochronal superposition and density scaling of the intermolecular dynamics in glass-forming liquids with varying hydrogen bonding propensity," RSC Adv. **6**, 49370 (2016).

[153] S. A. Khrapak, B. Klumov, L. Couedel, and H. M. Thomas, "On the long-waves dispersion in Yukawa systems," Phys. Plasmas **23**, 023702 (2016).

[154] P. Mausbach, A. Köster, G. Rutkai, M. Thol, and J. Vrabec, "Comparative study of the Grüneisen parameter for 28 pure fluids," J. Chem. Phys. **144**, 244505 (2016).

[155] M. Ozawa, K. Kim, and K. Miyazaki, "Tuning pairwise potential can control the fragility of glass-forming liquids: From a tetrahedral network to isotropic soft sphere models," J. Stat. Mech **2016**, 074002 (2016).

[156] M. Romanini, M. Barrio, R. Macovez, M. D. Ruiz-Martin, S. Capaccioli, and J. L. Tamarit,

"Thermodynamic scaling of the dynamics of a strongly hydrogen-bonded glass-former," Sci. Rep. **7**, 1346 (2017).

[157] G. Shrivastav, M. Agarwal, C. Chakravarty, and H. K. Kashyap, "Thermodynamic regimes over which homologous alkane fluids can be treated as simple liquids," J. Mol. Liq. **231**, 106–115 (2017).

[158] J. C. Dyre, "Hidden scale invariance in condensed matter," J. Phys. Chem. B **118**, 10007–10024 (2014).

[159] J. Daligault, "Liquid-state properties of a one-component plasma," Phys. Rev. Lett. **96**, 065003 (2006).

[160] M. Malvaldi and C. Chiappe, "Excess entropy scaling of diffusion in room-temperature ionic liquids," J. Chem. Phys. **132**, 244502 (2010).

[161] T. S. Ingebrigtsen, T. B. Schrøder, and J. C. Dyre, "What is a simple liquid?" Phys. Rev. X **2**, 011011 (2012).

[162] Y. Rosenfeld, E. Nardi, and Z. Zinamon, "Corresponding states hard-sphere model for the diffusion coefficients of binary dense-plasma mixtures," Phys. Rev. Lett. **75**, 2490–2493 (1995).

[163] R. Lalneihpuii, R. Shrivastava, and R. K. Mishra, "On the role of structure-dynamic relationship in determining the excess entropy of mixing and chemical ordering in binary square-well liquid alloys," Materials Research Express **5** (2018), 10.1088/2053-1591/aabec6.

[164] L. J. Lewis and G. Wahnström, "Molecular-dynamics study of supercooled ortho-terphenyl," Phys. Rev. E **50**, 3865–3877 (1994).

[165] L. Friedeheim, J. C. Dyre, and N. P. Bailey, "Hidden scale invariance at high pressures in gold and five other fcc metal crystals," arXiv:1810.07255 (2018).

[166] D. E. Albrechtsen, A. E. Olsen, U. R Pedersen, T. B. Schrøder, and J. C. Dyre, "Isomorph invariance of the structure and dynamics of classical crystals," Phys. Rev. B **90**, 094106 (2014).

[167] U. R. Pedersen, L. Costigliola, N. P. Bailey, T. B Schrøder, and J. C. Dyre, "Thermodynamics of freezing and melting," Nat. Commun. **7**, 12386 (2016).

[168] L. Costigliola, T. B. Schrøder, and J. C. Dyre, "Freezing and melting line invariants of the Lennard-Jones system," Phys. Chem. Chem. Phys. **18**, 14678 – 14690 (2016).

[169] T. B. Schrøder, N. Gnan, U. R. Pedersen, N. P. Bailey, and J. C. Dyre, "Pressure-energy

correlations in liquids. V. Isomorphs in generalized Lennard-Jones systems," J. Chem. Phys. **134**, 164505 (2011).

[170] L. Costigliola, T. B. Schrøder, and J. C. Dyre, "Communication: Studies of the Lennard-Jones fluid in 2, 3, and 4 dimensions highlight the need for a liquid-state 1/d expansion," J. Chem. Phys. **144**, 231101 (2016).

[171] L. Separdar, N. P. Bailey, T. B. Schrøder, S. Davatolhagh, and J. C. Dyre, "Isomorph invariance of Couette shear flows simulated by the SLLOD equations of motion," J. Chem. Phys. **138**, 154505 (2013).

[172] E. Lerner, N. P. Bailey, and J. C. Dyre, "Density scaling and quasiuniversality of flow-event statistics for athermal plastic flows," Phys. Rev. E **90**, 052304 (2014).

[173] A. A. Veldhorst, J. C. Dyre, and T. B. Schrøder, "Scaling of the dynamics of flexible Lennard-Jones chains: Effects of harmonic bonds," J. Chem. Phys. **143**, 194503 (2015).

[174] F. Hummel, G. Kresse, J. C. Dyre, and U. R. Pedersen, "Hidden scale invariance of metals," Phys. Rev. B **92**, 174116 (2015).

[175] A. A. Veldhorst, T. B Schrøder, and J. C. Dyre, "Invariants in the Yukawa system's thermodynamic phase diagram," Phys. Plasmas **22**, 073705 (2015).

[176] J. C. Dyre, "Isomorph theory of physical aging," J. Chem. Phys. **148**, 154502 (2018).

[177] D. Gundermann, U. R. Pedersen, T. Hecksher, N. P. Bailey, B. Jakobsen, T. Christensen, N. B. Olsen, T. B. Schrøder, D. Fragiadakis, R. Casalini, C. M. Roland, J. C. Dyre, and K. Niss, "Predicting the density–scaling exponent of a glass–forming liquid from Prigogine–Defay ratio measurements," Nat. Phys. **7**, 816–821 (2011).

[178] W. Xiao, J. Tofteskov, T. V. Christensen, J. C. Dyre, and K. Niss, "Isomorph theory prediction for the dielectric loss variation along an isochrone," J. Non-Cryst. Solids **407**, 190–195 (2015).

[179] K. Niss, "Mapping isobaric aging onto the equilibrium phase diagram," Phys. Rev. Lett. **119**, 115703 (2017).

[180] L. A. Roed, D. Gundermann, J. C. Dyre, and K. Niss, "Communication: Two measures of isochronal superposition," J. Chem. Phys. **139**, 101101 (2013).

[181] T. S. Ingebrigtsen, S. Toxvaerd, O. J. Heilmann, T. B. Schrøder, and J. C. Dyre, "NVU dynamics. I. Geodesic motion on the constant-potential-energy hypersurface," J. Chem. Phys. **135**, 104101 (2011).

[182] T. S. Ingebrigtsen, S. Toxvaerd, T. B. Schrøder, and J. C. Dyre, "*NVU* dynamics. II. Comparing to four other dynamics," J. Chem. Phys. **135**, 104102 (2011).

[183] T. S. Ingebrigtsen and J. C. Dyre, "*NVU* dynamics. III. Simulating molecules," J. Chem. Phys. **137**, 244101 (2012).

[184] A. K. Bacher, T. B. Schrøder, and J. C. Dyre, "Explaining why simple liquids are quasi-universal," Nat. Commun. **5**, 5424 (2014).

[185] A. K. Bacher, T. B. Schrøder, and J. C. Dyre, "The EXP pair-potential system. I. Fluid phase isotherms, isochores, and quasiuniversality," J. Chem. Phys. **149**, 114501 (2018).

[186] T. Maimbourg and J. Kurchan, "Approximate scale invariance in particle systems: A large-dimensional justification," EPL (Europhysics Letters) **114**, 60002 (2016).

[187] T. Young and H. C. Andersen, "A scaling principle for the dynamics of density fluctuations in atomic liquids," J. Chem. Phys. **118**, 3447–3450 (2003).

[188] K. Nagayama, *Introduction to the Grüneisen Equation of State and Shock Thermodynamics* (Amazon Digital Services, Inc., 2011).

[189] P. E. Ramirez-Gonzalez, L. Lopez-Flores, H. Acuna-Campa, and M. Medina-Noyola, "Density-temperature-softness scaling of the dynamics of glass-forming soft-sphere liquids," Phys. Rev. Lett. **107**, 155701 (2011).

[190] J. S. Rowlinson, "The statistical mechanics of systems with steep intermolecular potentials," Mol. Phys. **8**, 107–115 (1964).

[191] D. Henderson and J. A. Barker, "Perturbation theory of fluids at high temperatures," Phys. Rev. A **1**, 1266–1267 (1970).

[192] H. C. Andersen, J. D. Weeks, and D. Chandler, "Relationship between the hard-sphere fluid and fluids with realistic repulsive forces," Phys. Rev. A **4**, 1597–1607 (1971).

[193] H. S. Kang, S. C. Lee, T. Ree, and F. H. Ree, "A perturbation theory of classical equilibrium fluids," J. Chem. Phys. **82**, 414–423 (1985).

[194] K. R. Harris, "The selfdiffusion coefficient and viscosity of the hard sphere fluid revisited: A comparison with experimental data for xenon, methane, ethene and trichloromethane," Molec. Phys. **77**, 1153–1167 (1992).

[195] J. E. Straub, "Analysis of the role of attractive forces in self-diffusion of a simple fluid," Molec. Phys. **76**, 373–385 (1992).

[196] D. Ben-Amotz and G. Stell, "Reformulaton of Weeks–Chandler–Andersen perturbation the-

ory directly in terms of a hard-sphere reference system," J. Phys. Chem. B **108**, 6877–6882 (2004).

[197] A. E. Nasrabad, "Thermodynamic and transport properties of the Weeks–Chandler–Andersen fluid: Theory and computer simulation," J. Chem. Phys. **129**, 244508 (2008).

[198] T. Rodriguez-Lopez, J. Moreno-Razo, and F. del Rio, "Thermodynamic scaling and corresponding states for the self-diffusion coefficient of non-conformal soft-sphere fluids," J. Chem. Phys. **138**, 114502 (2013).

[199] J.-M. Bomont and J.-L. Bretonnet, "Thermodynamic scaling law for the diffusion coefficient in hard-sphere system," Physica A **420**, 23–27 (2015).

[200] P. V. Giaquinta, G. Giunta, and G. S. Prestipino, "Entropy and the freezing of simple liquids," Phys. Rev. A **45**, R6966–R6968 (1992).